Efficacy of Personalized Connectivity-Guided Accelerated Brain Stimulation in a Naturalistic Treatment-Resistant Depression Population

Ru Kong[1], Xiao Wei Tan[2], Aihuiping Xue[1], Leon Qi Rong Ooi[1], Shih Ee Goh[2], Jonathan Jie Lee[2], Jingwen Cheng[1], Trevor Wei Kiat Tan[1], Rachel Si Yun Tan[2], Jovi Zheng Jie Koh[2], Hasvinjit Kaur Gulwant Singh[2], Jia Hui Chai[3], Luming Shi[3], Shan Siddiqi[4,5], B.T. Thomas Yeo[1,6]*, Phern-Chern Tor[7]*

1. Centre for Sleep and Cognition (CSC) & Centre for Translational Magnetic Resonance Research (TMR), Yong Loo Lin School of Medicine, National University of Singapore, Singapore
2. Department of Mood & Anxiety, Institute of Mental Health, Singapore
3. Health Economics and Outcome Research, Singapore Clinical Research Institute, Consortium for Clinical Research and Innovation Singapore, Singapore
4. Department of Psychiatry, Mass General Brigham, Harvard Medical School, Boston, USA
5. Center for Brain Circuit Therapeutics, Brigham & Women's Hospital, Harvard Medical School, Boston, USA
6. Martinos Center for Biomedical Imaging, Massachusetts General Hospital, Charlestown, MA, USA
7. Department of Psychological Medicine, National University Hospital, Singapore

Keywords: Functional connectivity, treatment-resistant depression, intermittent theta burst stimulation, personalized target, cost-effectiveness

* Address correspondence to:
Phern-Chern Tor
Department of Psychological Medicine
National University Hospital
Email: Phern_chern_tor@nuhs.edu.sg

B.T. Thomas Yeo
CSC, TMR, ECE, N.1, WISDM
National University of Singapore
Email: thomas.yeo@nus.edu.sg

Abstract

Personalized connectivity-guided accelerated intermittent theta burst stimulation (iTBS), like the Stanford Accelerated Intelligent Neuromodulation Therapy (SNT), shows high efficacy for treatment-resistant depression (TRD) in Western cohorts. However, generalizability to other demographics with substantial comorbidity remains unclear. Here, we evaluate connectivity-guided iTBS in a naturalistic Asian TRD population with high comorbidity burden. Twenty TRD participants received 50 sessions of TAO-TMS (Tree-based Algorithm for Optimized Transcranial Magnetic Stimulation) over 5 days. Participants averaged 1.6 psychiatric comorbidities, including personality disorders, autism and obsessive–compulsive disorder. TAO-TMS personalizes targets within attentional networks and maximize anti-correlation with the subgenual anterior cingulate cortex. Its near-scalp targets reduce stimulation intensity under the SNT protocol, improving patient comfort. Clinical response was defined as ≥50% reduction in the Montgomery-Åsberg Depression Rating Scale within four weeks of treatment. TAO-TMS yielded 70% response rate. Among patients who met typical randomized-trial eligibility criteria (N = 11), response rate was 83%. For context, non-accelerated BeamF3 TMS at the same hospital historically achieved response rate of 21%, indicating a patient population profile less responsive to TMS than those recruited in typical clinical trials. Post-hoc electric-field modeling showed that TAO-TMS improved network focality by 21% over BeamF3 targets. Functional connectivity changes were significant within every participant, but highly heterogeneous across participants. TAO-TMS was more cost-effective than electroconvulsive therapy (ECT), saving US$37,838 with higher quality-adjusted life years (QALYs 0.69 vs 0.65). These findings provide early evidence for the generalizability of connectivity-guided personalized TMS in a naturalistic Asian TRD population with substantial psychiatric comorbidities. TAO-TMS offers a cost-effective alternative to ECT, positioning it as a viable precision psychiatry intervention.

Introduction

Treatment-resistant depression (TRD) is defined as major depressive disorder (MDD) that fails to respond to adequate trials of at least two antidepressant medications (Thase and Rush, 1997; Conway et al., 2017; Tor et al., 2022). 30% of patients with MDD is estimated to be treatment-resistant (Rush et al., 2006; McIntyre et al., 2023). TRD represents a significant public health burden due to its profound impact on quality of life and high healthcare utilization (Ho et al., 2013; Johnston et al., 2019; Chodavadia et al., 2023). Conventional pharmacological and psychotherapeutic approaches often prove insufficient for TRD, necessitating neurostimulation techniques, such as transcranial magnetic stimulation (TMS; George et al., 2013) or electroconvulsive therapy (ECT; Sackeim et al., 2001). TMS operates by inducing localized electric currents in brain tissues, modulating cortical excitability (Huerta and Volpe, 2009; Fox et al., 2012). Accelerated intermittent theta burst stimulation (iTBS), a more efficient variant of repetitive TMS, condenses sessions into shorter treatment windows, accelerating treatment timelines (Huang and Rothwell, 2004; Blumberger et al., 2018; Cole et al., 2020; Chu et al., 2021).

The therapeutic potential of TMS has been further advanced through individualized connectivity-guided targeting approaches (Fox et al., 2012; Liston et al., 2014; Bergmann et al., 2016; Cash et al., 2021; Siddiqi et al., 2021; Lynch et al., 2022; Hearne et al., 2025). Notably, the Stanford Accelerated Intelligent Neuromodulation Therapy (SNT) integrates personalized targets with a 5-day accelerated iTBS protocol, yielding exceptionally high response rates (Cole et al., 2020, 2022). However, such studies have primarily been conducted in carefully selected Western populations with relatively low comorbidity (Williams et al., 2018; Cole et al., 2020). Cross-ethnicity studies have shown systematic differences in resting-state brain organization (Li et al., 2022), which may affect stimulation targets and dosing (Kong et al., 2025; Zhang et al., 2025). Moreover, real-world TRD patients often present with comorbidities, polypharmacy, and variable episode durations – factors often excluded from tightly controlled trials. Consequently, the generalizability of these high-efficacy, accelerated, connectivity-guided paradigms to naturalistic clinical settings, particularly among ethnically diverse populations with substantial psychiatric comorbidity, remains under-explored (Jones et al., 2023).

To address these gaps, we applied our previously developed personalized targeting procedure, TAO-TMS (tree-based algorithm for optimized transcranial magnetic stimulation;

Kong et al., 2025), in an open-label trial of naturalistic treatment-resistant depression (TRD) patients in Singapore (NCT06341803). TAO-TMS targets exhibit higher reliability, closer scalp proximity and stronger anti-correlations to subgenual anterior cingulate cortex (Kong et al., 2025). The patient population examined here is clinically complex, characterized by high comorbidity, polypharmacy, and variable episode durations. Notably, a retrospective study from the same hospital reported a 21% response rate to non-accelerated BeamF3 TMS (Ye et al., 2024), suggesting that the present sample represents a population with lower historical TMS responsiveness than those commonly described in published studies.

Following the SNT protocol, each participant received 50 iTBS sessions (1,800 pulses; 10 sessions/day over 5 days) delivered using a neuro-navigated TMS system. As in SNT, stimulation intensity was adjusted using a linear ramp-down procedure. Because TAO-TMS provides near-scalp targets, our protocol further reduced stimulation intensity, improving tolerability and patient comfort. We additionally evaluated target precision via electric-field modeling, assessed pre-treatment to post-treatment functional connectivity changes, and performed a health-economic comparison of TAO-TMS and ECT. Overall, this study provides early evidence supporting the safety, efficacy, and mechanistic advantages of a SNT-like personalized neuromodulation protocol in an Asian cohort with complex TRD.

Methods and Materials

Participants and procedure

A preregistered open label trial was conducted at the Institute of Mental Health (IMH), Singapore (NCT06341803), from March 2024 to March 2025. Ethical approval was obtained (DSRB 2023/000397). Inclusion criteria were: (1) age ≥ 21; (2) DSM-5 diagnosis of MDD with current major depressive episode; (3) baseline Montgomery-Åsberg Depression Rating Scale (MADRS) ≥ 20; and (4) at least one failed antidepressant trial. Exclusion criteria included psychosis, recent substance abuse, acute suicidality requiring inpatient care, significant neurological disorders (e.g. epilepsy), pregnancy, or contraindications to magnetic resonance imaging (MRI) or transcranial magnetic stimulation (TMS). Participants maintained stable medications during the treatment week.

TMS treatment protocol

Stimulation was delivered with a MagPro X100 stimulator (MagVenture, Farum, Denmark). To ensure precise and reproducible coil placement, we utilized the Axilum Robotics TMS-Cobot (Axilum Robotics, Strasbourg, France) with the Localite neuronavigation system (Localite GmbH, Sankt Augustin, Germany). Real-time neuro-navigation was maintained to keep the coil within 2mm of the personalized target.

We employed the Stanford Accelerated Intelligent Neuromodulation Therapy (SNT) stimulation protocol. Each session delivered 1800 pulses consisting of bursts of 3 pulses at 50 Hz, repeated at 5 Hz, with a train duration of 2 seconds and an inter-train interval of 8 seconds. The coil (MagVenture Cool-B65) was positioned tangential to the scalp with the handle oriented at 45 degrees to the mid-sagittal line. Participants received 10 sessions per day over 5 consecutive days (50 sessions total). Sessions were separated by 50-minute inter-session interval.

Stimulation was delivered at 90% resting motor threshold (RMT), linearly adjusted for the cortical depth of the target relative to the motor hotspot (Stokes et al., 2005; Cole et al., 2020). To mitigate scalp discomfort, intensity was titrated from 70% to 90% of the adjusted RMT over the initial three sessions. Safety assessments, including RMT checks and adverse event monitoring, were conducted daily.

Clinical assessments and outcomes

Participants were assessed at baseline, post-treatment, 1-month and 3-month follow-ups using the MADRS score (Montgomery and Åsberg, 1979), Quick Inventory of Depressive Symptomatology (QIDS-SR16; Rush et al., 2003), Generalized Anxiety Disorder-7 (GAD-7; Spitzer et al., 2006), Montreal Cognitive Assessment (MoCA; Nasreddine et al., 2005), Sheehan Disability Scale (SDS; Sheehan et al., 1996), EuroQol-5D (EQ-5D; Group, 1990), and the Quality of Life Enjoyment and Satisfaction Questionnaire (Q-LES-Q-SF; Endicott et al., 1993). Daily QIDS-SR16 and GAD-7 scores were also collected at the end of each treatment day to capture short-term symptom changes. Efficacy analyses followed the intent-to-treat principle. The primary outcome was response (⩾50% reduction in MADRS) and remission (MADRS <11) within four weeks of acute treatment. Longitudinal effects were analyzed using repeated measures ANOVA and paired t-tests in SPSS v27 (IBM, Armonk, N.Y.). Details can be found in Supplementary Methods *Clinical assessments* and *Clinical outcome analysis*.

MRI acquisition & preprocessing

All MRI scans were acquired at the Centre for Translational Magnetic Resonance Research (TMR), National University of Singapore, on a 3T Siemens Prisma scanner. For each participant, a T1-weighted structural scan and two 10-minute resting-state fMRI (rs-fMRI) runs were collected prior to treatment. Acquisition details are provided in Supplementary Methods *MRI acquisition*. The scalp-based BeamF3 (Beam et al., 2009) stimulation location was also identified and marked on the scalp using a vitamin E capsule. Participants completed a second MRI session on average 5.0 ± 1.9 days after treatment, consisting of one T1-weighted structural scan and two resting-state fMRI runs. Data was preprocessed using the Computational Brain Imaging Group (CBIG) fMRI preprocessing pipeline (Li et al., 2019; Kong et al., 2025; Ooi et al., 2025). More details can be found in Supplementary Methods *fMRI preprocessing*.

Personalized TAO-TMS target

Personalized TAO-TMS target in the left dorsolateral prefrontal cortex (DLPFC) was generated for each participant using baseline rs-fMRI. To preserve individual anatomical fidelity, localization was performed in the participant's native volumetric space. We employed the Multi-Session Hierarchical Bayesian Model (MS-HBM) to estimate reliable individual-specific cortical networks (Kong et al., 2019), which were then mapped into the participant's native volumetric

space. A tree-based algorithm was then used to estimate a personalized target within attentional networks in left DLPFC that exhibited the strongest negative functional connectivity (FC) with the subgenual anterior cingulate cortex (sACC), while remaining close to the scalp to minimize TMS intensity requirements (Kong et al., 2025). The attentional networks were chosen because dorsal attention and salience/ventral attention networks are known to be negatively correlated with the default network (Fox et al., 2006) and thus the sACC time course (Siddiqi et al., 2023). We also note that the salience network has been shown to be enlarged in depression patients (Lynch et al., 2024).

TMS-induced electric field

To evaluate the precision of personalized TAO-TMS targets relative to standard scalp-based localization, we compared the electric field (E-field) properties of the TAO-TMS target with the BeamF3 location (Beam et al., 2009). Individualized head models were generated from the anatomical MRI scans using SimNIBS 4.1.0 (Thielscher et al., 2015). For each participant, we simulated the E-field distribution for both the administered personalized target and the BeamF3 target (derived from the MRI-visible fiducial marker) using the MagVenture Cool-B65 coil model with coil angle 45 degree. For each simulation, the "E-field hotspot" was defined as the set of cortical vertices representing the top one percent of E-field magnitude (Lynch et al., 2022; Ren et al., 2025).

To assess target quality, two evaluation metrics were considered. First, network specificity was defined as the percentage of the E-field hotspot area occupied by the target networks (dorsal and salience/ventral attention networks). Second, we computed the FC between the E-field hotspot and the sACC (Fox et al., 2013; Cash et al., 2021; Elbau et al., 2023) at baseline. More specifically, a rs-fMRI time course was computed based on a weighted average of DLPFC vertices' time courses, where the weights corresponded to the local E-field strength. The DLPFC time course was then correlated with the sACC time course. A more negative hotspot sACC FC might indicate better target quality (Weigand et al., 2018; Elbau et al., 2023).

Treatment-related functional connectivity changes

For participants with both pre-treatment and post-treatment scans, the difference in hotspot sACC FC (post-treatment minus baseline) was correlated with the percentage

improvement in MADRS scores. To examine whole-brain FC changes, for each participant, two 419 x 419 FC matrices were computed – one at baseline and one post-treatment – with 400 cortical (Schaefer et al., 2018) and 19 subcortical (Fischl, 2012) regions. FC was computed using xDF (Afyouni et al., 2019). xDF accounts for fMRI temporal autocorrelation, which allowed us to compute a z-statistic for FC change (post-treatment minus baseline) for every FC edge of each individual. Multiple comparisons were corrected with a false discovery rate (FDR) of $q < 0.05$.

Exploratory analyses of coil orientation and target constraints on clinical efficacy

To assess whether optimization of stimulation parameters could further enhance clinical outcomes, we conducted two sets of exploratory analyses. First, the coil orientation in our trial was set to be 45 degrees, following the SNT protocol. Here, we examined whether optimizing the coil angle could potentially improve clinical outcomes. For each participant, we changed the coil orientation to maximize hotspot sACC FC. The differences between the maximum hotspot sACC FC and the actual hotspot sACC FC (based on the 45 degrees coil angle) were then correlated with clinical improvement across participants. A negative correlation would suggest that optimizing coil orientation to maximize hotspot sACC FC might potentially improve clinical outcomes. We repeat the same analysis by replacing hotspot sACC FC with attentional network specificity.

Second, recall that TAO-TMS restricted the target to be near the scalp and to be within the attention networks. Here, we evaluated the impact of these restrictions on clinical outcomes. More specifically, personalized TMS targets were regenerated without the near-scalp constraint, and the Euclidean distance between these unconstrained targets and the original targets was correlated with MADRS improvement. A negative correlation would suggest that the near-scalp constraint was potentially worsening clinical outcomes. The same analysis was repeated by turning off both the near-scalp and attentional network constraints.

Health Economic Evaluation

We conducted a cost-effectiveness analysis comparing TAO-TMS with ECT using a standard hybrid decision tree–Markov model over a one-year time horizon (Figure S1; Sonnenberg and Beck, 1993). Analyses were performed from both healthcare system and societal perspectives. EQ-5D utilities were converted into quality-adjusted life years (QALYs;

Drummond et al., 2015), and costs included TMS, imaging, medication, adverse events, and productivity loss. Incremental cost-effectiveness ratios (ICERs) were calculated (Weinstein et al., 1996), and uncertainty was assessed using one-way sensitivity analyses and probabilistic sensitivity analyses with 10,000 Monte Carlo simulations (Briggs, 1999; Briggs et al., 2006). From these simulations, cost-effectiveness acceptability curves (CEACs) were generated to show the probability that TAO-TMS is more cost-effective than ECT across a range of willingness-to-pay thresholds. Scenario analyses examined shorter time horizons and conservative model structures. Full methodological details are provided in the Supplementary Methods *Health Economic Evaluation*. All costs were analyzed in 2025 Singapore Dollars (SGD) and are also presented in US Dollars (USD) using a fixed exchange rate of 1 USD = 1.29 SGD.

Results

Study population and safety

Figure 1 shows the CONSORT flow diagram. Of 27 participants screened, 21 participants were recruited (mean age 35.1 years; 57.1% female; 81% Chinese, 19% South Asian). The sample exhibited substantial clinical complexity (Table 1), with 86% meeting criteria for at least one additional psychiatric diagnosis, an average of 4.7 failed antidepressant trials, and 19% having previously received electroconvulsive therapy (ECT). One participant discontinued treatment early due to discomfort, resulting in a final sample of 20 participants who completed the full treatment protocol. Detailed demographic and clinical characteristics are summarized in Table S1.

The final treated cohort had a mean age of 35.1 ± 12 years with high baseline disease severity (MADRS = 28.3 ± 5.1; failed antidepressant trials 4.7 ± 2.3). One participant withdrew after four TMS sessions, while 20 participants completed the full treatment course of fifty sessions. Among the 20 participants, average number of comorbid psychiatric diagnoses was 1.7. Only three participants had no comorbid psychiatric diagnosis. No serious adverse events occurred, and the robotic TAO-TMS protocol was confirmed to be safe and well-tolerated across the participants.

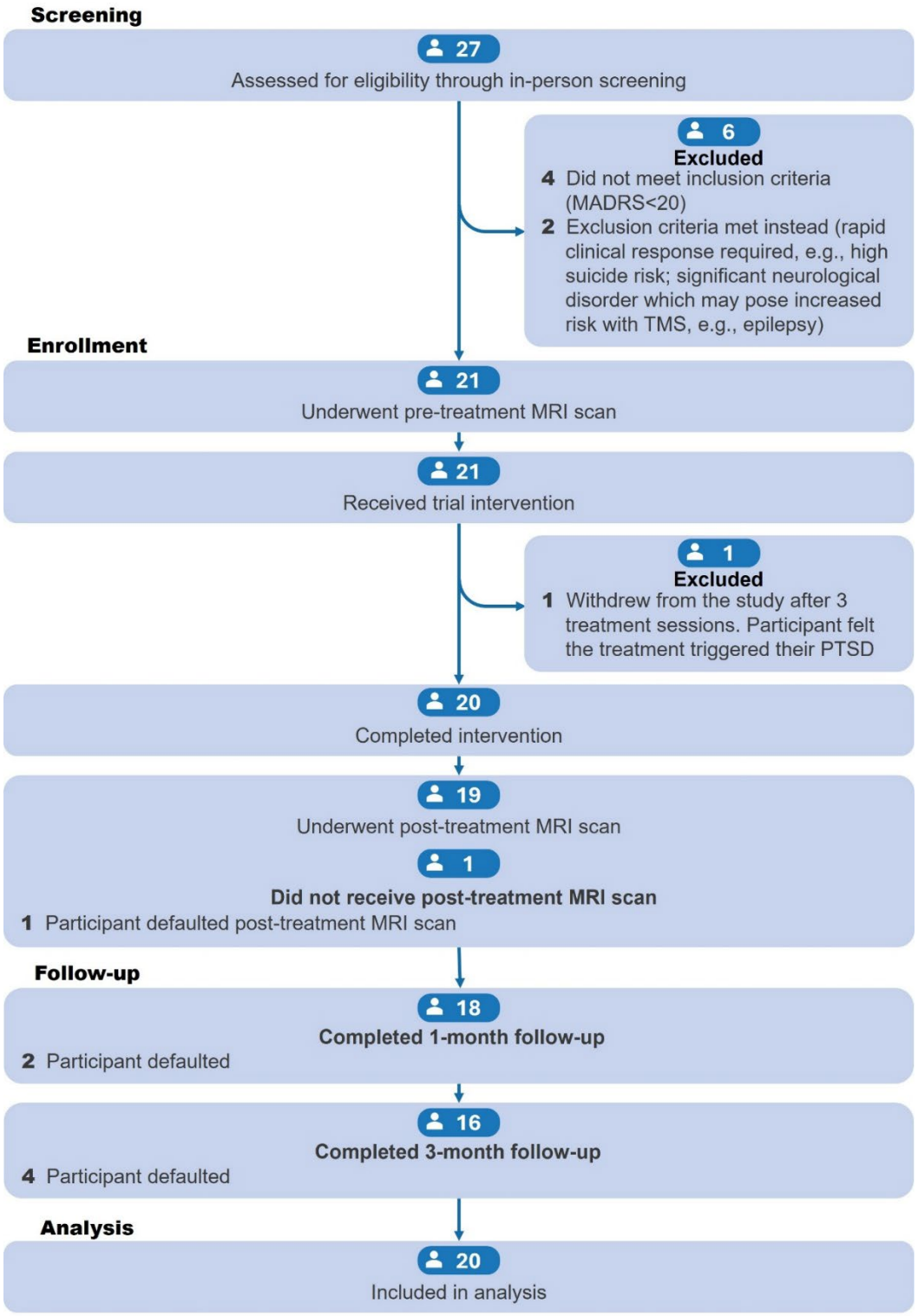

Figure 1. CONSORT flow diagram.
TMS, transcranial magnetic stimulation; MADRS, Montgomery-Asberg Depression Rating Scale; PTSD, post-traumatic stress disorder; MRI, magnetic resonance imaging.

Table 1. Baseline demographic and clinical characteristics of all intent-to-treat participants.

Baseline characteristic	Participants (N=21)
Age, years, mean (SD)	35.14 (12.25)
Gender, No. (%)	
Male	9 (43)
Female	12 (57)
Ethnicity, No. (%)	
Chinese	17 (81)
South Asian	4 (19)
Comorbidities, No. (%)	
Generalized anxiety disorder	12 (57)
Post-traumatic stress disorder	6 (29)
Personality disorder	6 (29)
Feeding and eating disorder	5 (24)
Autism spectrum disorder	3 (14)
Bipolar disorder II	1 (5)
Attention-deficit/hyperactivity disorder	1 (5)
Obsessive-compulsive disorder	1 (5)
Gender dysphoria with affirmative surgery	1 (5)
Breast and kidney cancer	1 (5)
Hepatitis B	1 (5)
Number of failed antidepressants trials, mean (SD)	4.67 (2.27)
Past ECT treatment, No. (%)	4 (19)
Past TMS treatment, No. (%)	8 (38)
Clinical assessments, mean (SD)	
MADRS	28.33 (5.14)
QIDS-SR16	20.67 (6.45)
GAD-7	10.86 (5.26)
Q-LES-Q-SF	39.00 (9.64)
EQ-5D-3L utility score	0.39 (0.33)
SDS total score	17.86 (6.46)
MoCA	28.52 (1.47)

ECT, electroconvulsive therapy; TMS, transcranial magnetic stimulation; MADRS, Montgomery-Asberg Depression Rating Scale; QIDS-SR16, The Quick Inventory of Depressive Symptomatology (16-Item) (Self-Report); GAD-7, Generalized Anxiety Disorder-7 item; Q-LES-Q-SF, Quality of Life Enjoyment and Satisfaction Questionnaire-Short form; EQ-5D-3L, EuroQol 5-dimensional questionnaire with 3-levels; SDS, Sheehan Disability Scale; MoCA, the Montreal Cognitive Assessment.

Personalized TAO-TMS targets

TAO-TMS was used to derive a personalized target in each participant's native T1 volumetric space using baseline rs-fMRI. Figure 2A illustrates the spatial distribution of personalized targets overlaid on group-level cortical networks (Yeo et al., 2011; Kong et al., 2019). Participants exhibited highly distinct network topography (Figure 2B top panel). All

TAO-TMS target locations were close to the scalp (Figure 2B bottom panel) with an average distance of 14.1 mm from the scalp as measured in native volumetric space. The mean pairwise distance between the personalized targets across the 20 participants was 9.6 mm (Figure 2C). For context, the mean distance between the personalized TAO-TMS targets and the traditional scalp-based BeamF3 targets was 13.4 mm (Figure 2D), with a maximum deviation of 31.5 mm. The considerable deviation highlights the potential for suboptimal target engagement when relying solely on anatomical landmarks rather than individualized functional connectivity.

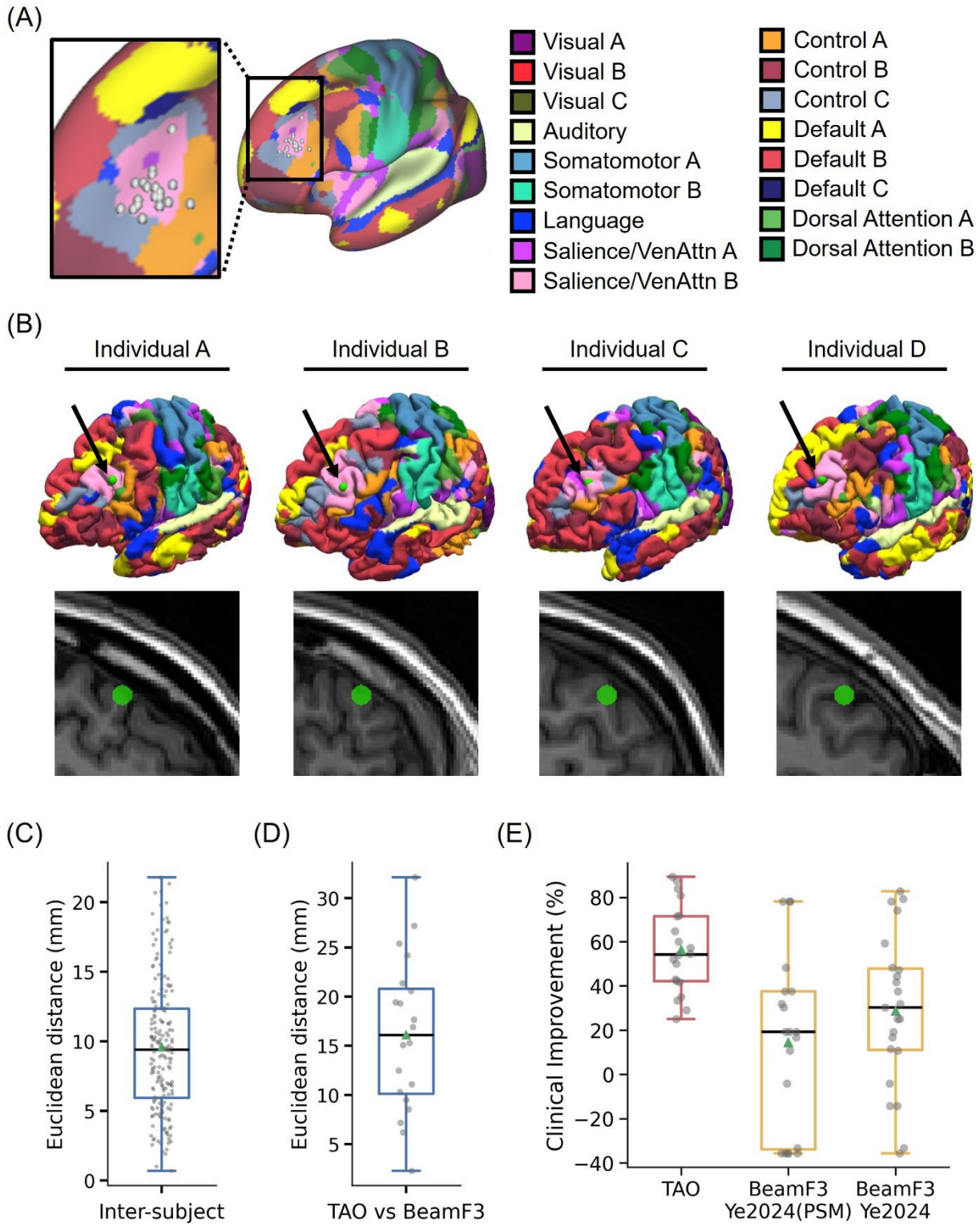

Figure 2. Comparison of TAO-TMS and BeamF3 targets (A) Personalized depression targets of 20 participants overlaid on a group-level map of 17 resting-state networks (Yeo et al., 2011; Kong et al., 2019). Target locations were estimated in each participant's native T1 volumetric space using baseline rs-fMRI and then projected to fsaverage6 surface space for visualization.

(B) TAO-TMS targets are situated within personalized attention networks and are located close to the scalp. Four representative participants are shown here, with targets (green circles) displayed on native pial surfaces (top) and native T1 images (bottom). Black arrows point to the green circles on the native pial surfaces. A target located deep within a sulcus would not be visible on the native pial surface, so the visible targets (green circles) indicate that TAO-TMS was able to successfully localize near-scalp targets. (C) Boxplot of the pairwise distances between the personalized targets across the 20 participants. (D) Boxplot of the distances between the personalized targets and the scalp-based BeamF3 targets across 20 participants. (E) Clinical improvement of TAO-TMS (N = 20), and a retrospective analysis of non-accelerated BeamF3 TMS at the same hospital (N = 23; # sessions = 49 ± 29; Ye et al., 2024). Boxplots show percentage reduction in MADRS scores immediately after treatment. Positive values indicate greater improvement. Females were over-represented in the Ye2024 study, so the middle boxplot "BeamF3 Ye2024 (PSM)" shows the clinical improvement of a subsample of participants that were propensity-matched (in terms of age and sex) to the TAO-TMS trial.

Efficacy of TAO-TMS

Participants demonstrated robust clinical improvement, with MADRS reduction of 57% ± 19% (N = 20; Figure 2E). For context, a retrospective analysis of non-accelerated BeamF3 TMS at the same hospital found a MADRS reduction of 29% ± 34% (N = 23) with a comparable number of TMS sessions = 49 ± 29 (Ye et al., 2024). Females were over-represented in the Ye2024 sample. A subsample of participants that were propensity-matched (in terms of age and sex) to the TAO-TMS trial exhibited a MADRS reduction of 14% ± 40% (Figure 2E). Although these studies differ in design and cannot be directly compared, the trend suggests that personalized targeting may hold promise for improving treatment outcomes.

The primary TAO-TMS outcome, MADRS response rate within one month after acute treatment, was 70% (Figure 32A; Table S2) with a large effect size (Cohen's $d = 2.2$; Table S3). Response and remission rates immediately after acute treatment, at 1-month and 3-month follow-ups, were 65%/30%, 50%/27.8%, and 31.3%/6.3%, respectively (Figure 3A; Table S2). MADRS scores remained significantly lower at both 1-month and 3-month follow-ups compared to baseline (Figure 3A). Improvements in QIDS-SR and GAD-7 largely paralleled MADRS changes (Figure S2), although GAD-7 scores were not significantly different from baseline at 1-month and 3-month follow-ups (Figure S2; Table S3).

Functional outcomes also improved following TAO-TMS. SDS scores decreased, reflecting a reduction in days lost from 3.6 to 1.8, and EQ-5D utility increased from 0.39 to 0.60 post-treatment (Table S2). MoCA scores remained stable, indicating preserved cognitive function

(Table S2). Throughout the treatment course, the personalized targets were delivered reliably, with a mean deviation of 1.8 ± 0.7 mm (Figure 3B).

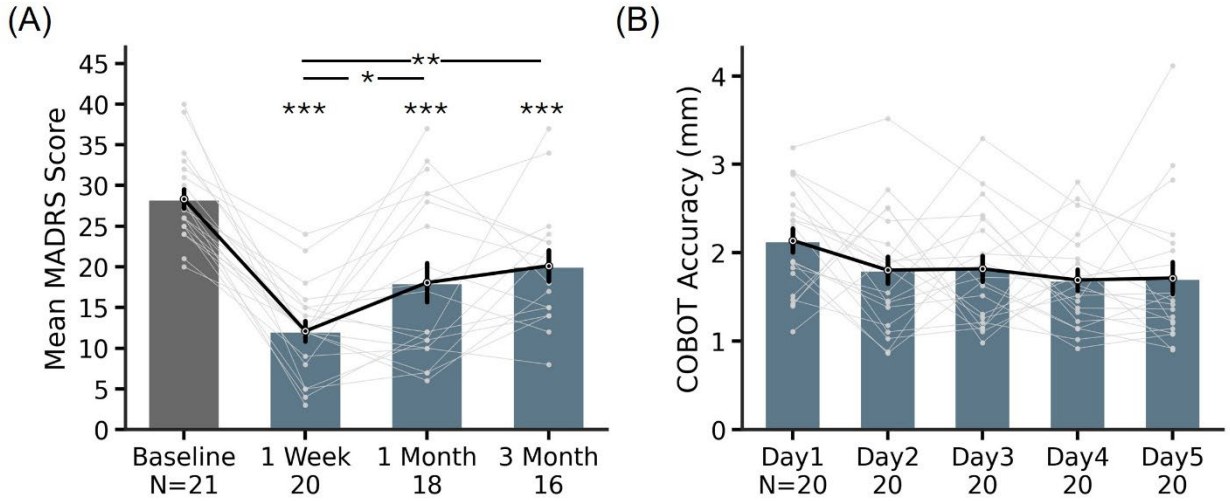

Figure 3. Clinical outcomes and treatment delivery accuracy. (A) Mean MADRS scores at baseline, post-acute treatment (1 week), 1-month, and 3-month follow-up. * indicates statistical significance after multiple comparisons correction with FDR q < 0.05. *p<0.05. **p<0.01. ***p<0.001. (B) COBOT accuracy for personalized TAO-TMS target delivery across the five treatment days, expressed as the mean Euclidean distance between the actual stimulation site and the planned stimulation site. Error bars represent standard error.

E-field characteristics of TAO-TMS vs BeamF3 targets

TAO-TMS selects a personalized target within attentional networks in left DLPFC that exhibited the strongest negative FC with sACC. Therefore, unsurprisingly, TAO-TMS targets produced a 21.4% stronger on-target E-field engagement of attentional networks compared with the scalp-based BeamF3 targets (p = 0.012; Figures 4A and 4B). Figure S3 shows the E-field hotspot network engagement for TAO-TMS and BeamF3 targets for different networks. As expected, the E-field hotspot of TAO-TMS targets also exhibited an 87.6% stronger (more negative) hotspot sACC FC than BeamF3 targets at baseline (p = 0.012; Figure 4C). These results suggest that TAO-TMS targets might more strongly modulate the attentional networks and the sACC circuit.

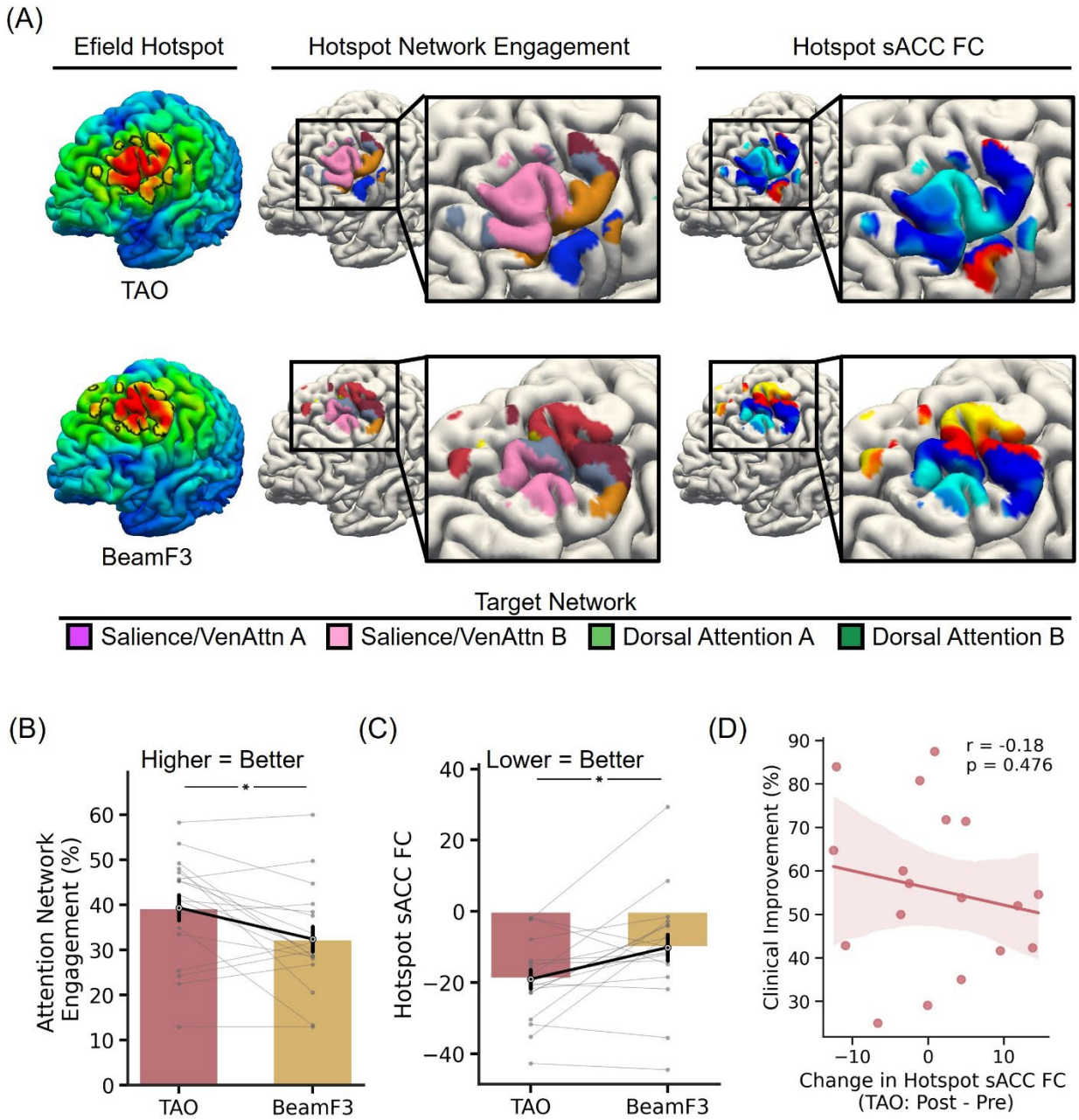

Figure 4. Electric field characteristics of TAO-TMS and BeamF3 targets. (A) E-field characteristics of TAO-TMS target (top row) and BeamF3 target (bottom row) in a representative participant. The left panel shows the E-field maps estimated using SimNIBS, with the "E-field hotspot" defined as the top 1 percent of cortical vertices (black boundaries) following previous studies (Lynch et al., 2022; Ren et al., 2025). The middle panel shows the personalized MS-HBM networks within the E-field hotspot The right panel shows functional connectivity between the E-field hotspot and the sACC. Target networks are the salience/ventral attention networks A and B and dorsal attention networks A and B. (B) Comparison of TAO-TMS and BeamF3 targets in terms of attentional network E-field engagement across 20 participants. Higher values indicate greater engagement of the target networks. (C) Comparison of TAO-TMS targets and BeamF3 targets in terms of hotspot sACC FC across 20 participants. Lower values indicate stronger

anticorrelation with sACC. (D) Association between clinical improvement (percentage MADRS reduction) and the change in hotspot sACC FC from pre-treatment to post-treatment. There were 18 participants in this plot because one missed the post-treatment scan and one was excluded due to excessive motion

Treatment-related functional connectivity changes

Of the 20 participants who completed treatment, one missed the post-treatment scan and one was excluded due to excessive motion, leaving 18 participants for the following analyses. We investigated whether clinical efficacy related to FC changes pre-treatment and post-treatment in 18 participants. Recall that two participants were excluded due to one missing the post-treatment scan and the other due to excessive motion. We remind the readers that the E-field hotspot (top row in Figure 4A) corresponded to the actual simulation hotspot. There was no significant correlation between percentage MADRS reduction and change in hotspot sACC FC ($r = -0.18$, $p = 0.476$; Figure 4D).

At the whole-brain level, there were statistically significant alterations in whole-brain functional connectivity in every participant, but the spatial patterns of these changes were highly heterogeneous across participants (Figure 54; Figures S4 to S6). Qualitatively, responders might exhibit greater FC changes, but this was not statistically significant. We note that among the non-responders, one participant displayed substantial FC changes post-treatment and subsequently showed clinical response at the 3-month follow-up (non-responder 4 in Figures S5 to S6).

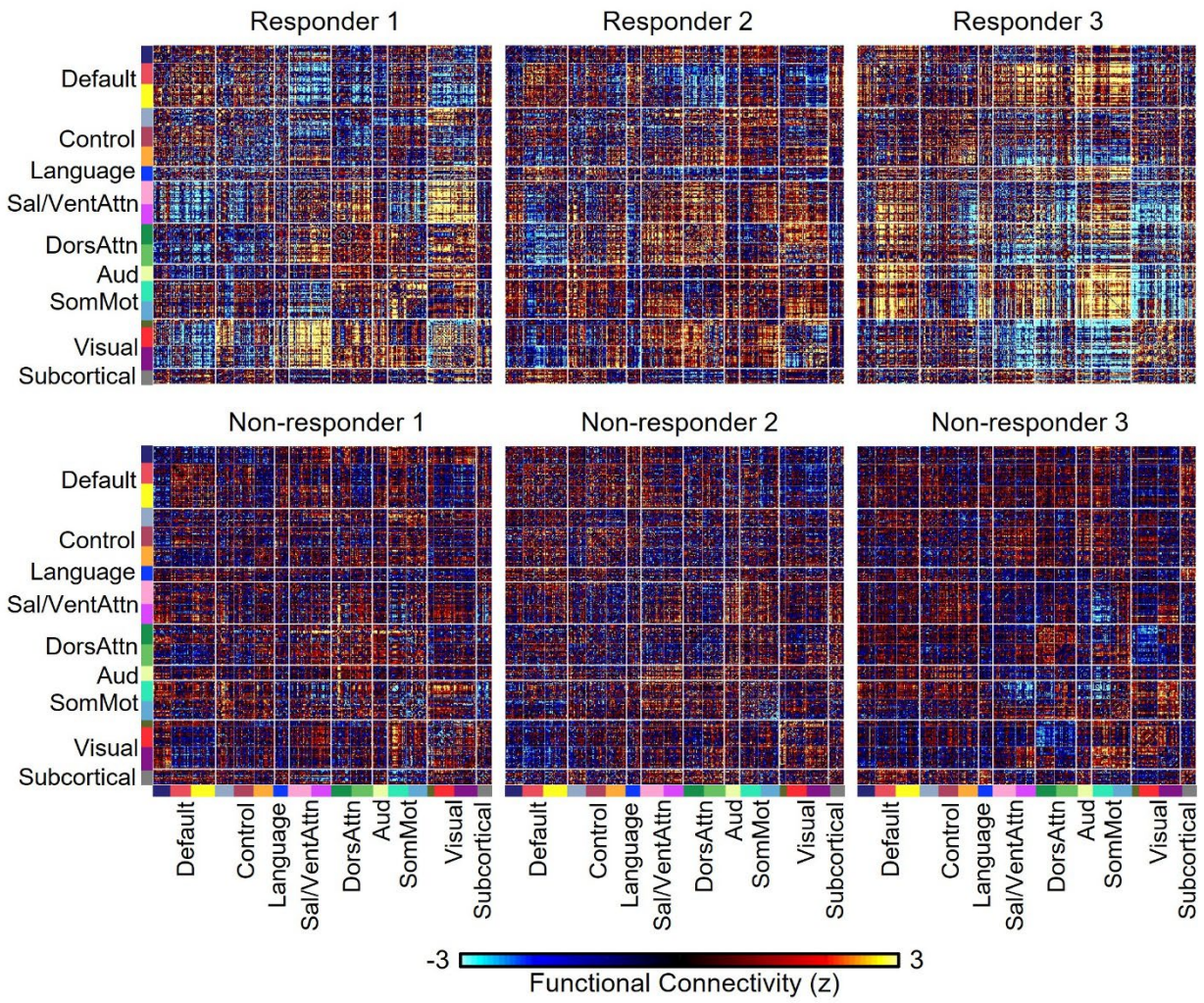

Figure 5. Functional connectivity (FC) changes pre-treatment and post-treatment TAO-TMS. Top panel shows three responders, while bottom panel shows three non-responders. Figure S4 shows thresholded FC changes after FDR correction ($p < 0.05$). FC changes of remaining participants are shown in Figures S5 to S6.

Impact of coil orientation & target constraints on clinical efficacy

Following the SNT protocol, coil angle was oriented was 45 degrees. Here we performed post hoc exploratory analysis to examine whether optimizing coil orientation could further improve clinical efficacy. Differences in on-target attentional network engagement between optimal coil angle and actual coil angle (45 degrees) were not correlated with clinical efficacy ($r = -0.35$; $p = 0.16$; Figure S7A). Similarly, differences in hotspot sACC FC between optimal coil angle and actual coil angle (45 degrees) were also not correlated with clinical efficacy ($r = 0.14$;

p = 0.59; Figure S7B). With the small sample size in mind, these findings suggest that additional optimization of coil angle may not yield further gains in clinical efficacy.

Furthermore, recall that TAO-TMS restricted the target to be near the scalp and within the attention networks. Post hoc analysis suggests that relaxing the near-scalp constraint would not further improve clinical efficacy (r = -0.18; p = 0.46; Figure 6A). Relaxing both near-scalp and attentional network constraints also would not improve clinical efficacy (r = –0.08; p = 0.73; Figure 6B).

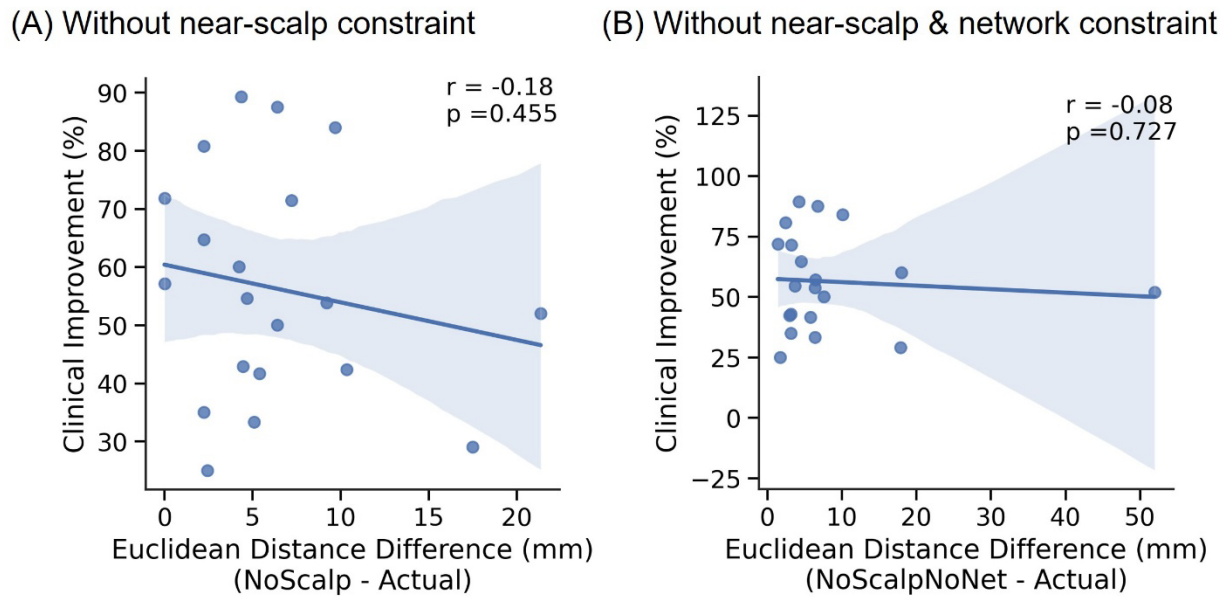

Figure 6. Post hoc exploratory analysis of TAO-TMS target constraints. (A) Correlation of percentage MADRS reduction with the distance of personalized targets generated without the near-scalp constraint and actual TAO-TMS targets. A negative correlation would suggest that the near-scalp constraint was hurting clinical efficacy. (B) Correlation of percentage MADRS reduction with the distance of personalized targets generated without both the near-scalp and attentional network constraints and actual TAO-TMS targets. A negative correlation would suggest that the near-scalp constraint was hurting clinical efficacy. Neither correlation reached statistical significance.

Health Economic Outcomes

TAO-TMS demonstrated favorable economic outcomes compared with electroconvulsive therapy (ECT). From the health system perspective, TAO-TMS reduced costs by S$12,284 (US$9,523), with total costs of S$43,483 (US$33,708) versus S$55,767 (US$43,231) for ECT, while also achieving a higher quality-adjusted life years (QALYs): 0.69 vs 0.65. From the

societal perspective, which includes productivity losses, TAO-TMS produced an even greater savings of S$36,527 (US$28,316). Full results are provided in Table S5.

Cost-effectiveness acceptability curves (Figure 7) show that across a wide range of willingness-to-pay thresholds, TAO-TMS consistently maintained a high probability of being cost-effective compared with ECT. One-way sensitivity analyses indicated that TAO-TMS would lose dominance only if ECT costs fell below S$361.5 (US$280.3), whereas the societal perspective remained robust to all parameter variations (Figure S8).

Shorter time horizons modestly reduced the magnitude of cost-effectiveness, but TAO-TMS remained the preferred option (Table S6). Conservative scenario modeling using a simplified two-state Markov model also supported TAO-TMS as the preferred option (Table S7; see Figure S9 for the decision analytical model). Further details can be found in Supplementary Results *Cost-effectiveness analysis*.

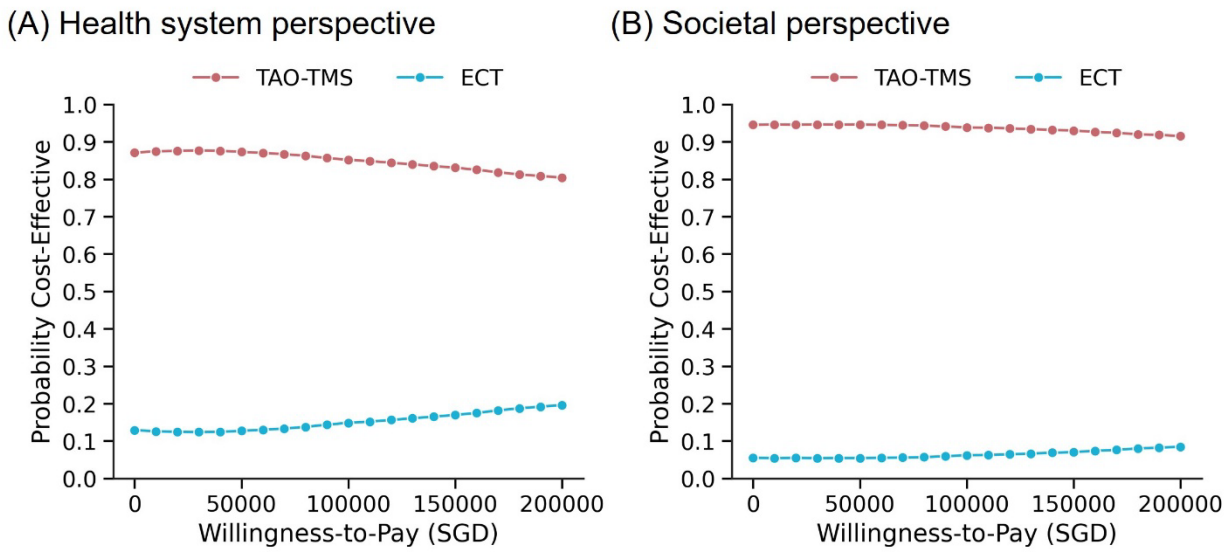

Figure 7. Cost-effectiveness acceptability curves for TAO-TMS versus ECT. The probability that TAO-TMS was cost-effective compared with ECT across a range of willingness-to-pay thresholds from (A) the health system perspective and (B) the societal perspective, which includes productivity losses. TAO-TMS consistently demonstrates a high probability of being cost-effective across all thresholds. Note that US$1 ≈ S$1.29.

Discussion

This is one of the first studies evaluating connectivity-guided accelerated iTBS in an Asian TRD population with high comorbidity burden. TAO-TMS demonstrated 70% response rate, which is three times the historical response rate of 21% with non-accelerated BeamF3 TMS from the same hospital (Ye et al., 2024). Post hoc E-field analysis confirmed that TAO-TMS exhibited 21.4% stronger engagement of attentional networks and 87.6% stronger (more negative) hotspot sACC FC than BeamF3. There were significant FC changes within each individual, but the study was not sufficiently powered to find any relationship between FC changes and treatment response. Finally, TAO-TMS was more cost-effective than ECT, saving US$37,838 with QALYs.

Effects of psychiatric comorbidities and target personalization on clinical efficacy

The original SNT open-label trial reported >90% response and remission rates (Cole et al., 2020)[1]. In contrast, our TAO-TMS cohort was more naturalistic, with many participants presenting psychiatric comorbidities such as personality disorders, autism, or obsessive–compulsive disorder (OCD) – conditions typically excluded from randomized MDD trials (Sforzini et al., 2022). Psychiatric complexity therefore likely contributed to the lower overall response we observed.

This pattern is reflected in the broader literature. In accelerated iTBS trials using anatomical/scalp targets, naturalistic Western cohorts with complex psychiatric comorbidities reported lower response rates than studies excluding such patients: 25%-28% (Goodman et al., 2025; Persson et al., 2025) vs 52%-75% (Luehr et al., 2024; Zhao et al., 2024; Ramos et al., 2025).

Stronger evidence comes from trials directly comparing patients with and without comorbidities. An Australian study found that unaccelerated connectivity-guided iTBS yielded a 74% response rate in trial-eligible patients versus 44% in those with complex comorbidities (Hearne et al., 2025). Consistently, in our TAO-TMS sample, excluding participants with autism, OCD, personality disorders or gender dysphoria increased response to 83%, whereas participants

[1] A Chinese study (Li et al., 2024) also reported high remission and response with a SNT-like protocol, but direct comparison is limited because (i) participants with psychiatric comorbidities were excluded, (ii) antidepressants were discontinued for ≥2 months before enrollment, and (iii) venlafaxine/duloxetine was initiated at TMS onset.

with these comorbidities showed a response rate of 50%. These within-study contrasts provide relatively strong evidence that psychiatric comorbidities substantially diminish treatment response.

On the other hand, when comparing trials involving naturalistic populations, connectome-guided iTBS (TAO-TMS; Hearne et al., 2025) appeared to yield higher clinical efficacy than anatomical/scalp-targeted iTBS (Goodman et al., 2025; Persson et al., 2025): response rates 46%/70% vs 25%/28%, and remission rates 30%/33% vs 16%/17%. This pattern suggests that individualized sACC-connectivity-guided targeting may offer clinical advantages even in complex real-world populations. However, unlike the comorbidity comparison, these observations rely on cross-study rather than within-study contrasts. A definitive test of whether connectome-guided targeting outperforms anatomical/scalp-based approaches will require head-to-head clinical trials.

TMS-related functional connectivity

In our study, FC changes between the stimulation site and the sACC did not significantly correlate with symptom improvement. At the whole-brain level, we observed significant FC changes within each individual. The FC changes were highly variable across individuals, and were not associated with treatment response. This large heterogeneity is potentially due to many participants presenting complex psychiatric comorbidities. Therefore, a larger sample size would be necessary to fully disentangle baseline psychiatric heterogeneity and FC changes related to treatment response.

It is also worth noting that a recent review suggested that the relationship between TMS-related FC changes and symptom improvement has mixed evidence in the literature (Briley et al., 2024). Some studies have reported significant associations between TMS-related FC changes and symptom improvement (Philip et al., 2018; Eshel et al., 2020; Oathes et al., 2023), while other studies reported weak or non-significant associations (Ge et al., 2022; Stöhrmann et al., 2023; Jin et al., 2025). Together, these findings highlight the need for larger sample sizes to clarify the relationship between TMS-related FC changes and clinical response.

Health economics: policy and system-level implications

Health economic analyses indicate that TAO-TMS is more cost-effective than ECT from both payer and societal perspectives. This is particularly relevant in Singapore and other Asian settings, where ECT remains common, but carries stigma, cognitive risks, and higher indirect costs from hospitalization and recovery (Zhao et al., 2018; Fitzgibbon et al., 2020). In contrast, TAO-TMS is outpatient-based, preserves cognition, and requires minimal downtime, reducing direct expenditures and productivity losses.

From a health system perspective, TAO-TMS saved US$9,500 per patient compared to ECT. From a societal perspective, savings exceeded US$28,000. These numbers are substantial when scaled to TRD prevalence, which is estimated to be 30% of patients with MDD (Rush et al., 2006; McIntyre et al., 2023). For policy makers, this positions TAO-TMS as a high-value intervention, especially in middle-income countries balancing resource constraints and mental health priorities.

Our sensitivity analyses underscore robustness: only when ECT costs drop unrealistically low (< US$280) would TAO-TMS lose dominance. Probabilistic simulations confirmed >95% likelihood of cost-effectiveness at willingness-to-pay thresholds aligned with Singapore gross domestic product (GDP) per capita. Importantly, our analyses incorporated indirect costs, often overlooked in payer-focused models, but critical in regions where depression disproportionately affects working-age adults.

These findings align with previous Singapore health technology assessments (Zhao et al., 2018; Teng et al., 2021) and with economic evaluations from North America (Kozel et al., 2004; Fitzgibbon et al., 2020) and Europe (Zemplényi et al., 2022), but extend them by including accelerated, connectivity-guided TMS, a modality not yet widely assessed in formal cost-effectiveness frameworks.

Limitations

Our small sample size offered limited statistical power for subgroup analyses, such as comorbidity or prior ECT. Another key limitation of our study is the lack of a placebo arm or anatomical/scalp-based target as an active control.

In addition, some studies have suggested that e-field modeling might improve personalized target selection (Weis et al., 2020; Lynch et al., 2022; Deng et al., 2023; Elbau et

al., 2023; Lueckel et al., 2023; Dannhauer et al., 2024; Sun et al., 2024). Although our tree-based algorithm could also include e-field modeling, the current TAO-TMS did not.

However, we retrospectively examined whether optimizing coil orientation using E-field modeling could improve clinical improvement. These analyses did not reveal meaningful benefits, but this negative finding may be limited by our small sample size. Future studies with larger samples and randomized controlled designs are needed to determine whether integrating E-field modeling can enhance target precision and therapeutic efficacy.

Conclusions

This study provides an early demonstration that connectivity-guided TMS may be effective in naturalistic Asian TRD populations with higher comorbidity burden. Given its favorable cost profile compared with ECT, TAO-TMS merits further validation as a precision-psychiatry intervention in larger controlled trials.

Author Contributions

RK, XWT, AX, LQRO, SEG, JL, TWKT, RSYT, JZJK, HKGS, PCT contributed to IMH and NUS which generated data for this report. RK, XWT, JC, RSYT, JZJK, JHC, and LS analyzed the data. RK, BTTY and PCT wrote the first draft of the manuscript. All authors edited the manuscript.

Acknowledgements

The authors would like to acknowledge the support of the Temasek Foundation Climate and Livability Board, the team from the Neurostimulation Service, Institute of Mental Health (Singapore) and our patients and families. Our research is supported by the NUS Yong Loo Lin School of Medicine (NUHSRO/2020/124/TMR/LOA), the Singapore National Medical Research Council (NMRC) LCG (OFLCG19May-0035), NMRC CTG-IIT (CTGIIT23jan-0001), NMRC OF-IRG (OFIRG24jan-0006; OFIRG24jul-0049), NMRC STaR (STaR20nov-0003), Singapore Ministry of Health (MOH) Centre Grant (CG21APR1009), the Temasek Foundation (TF2223-IMH-01), the United States National Institutes of Health (R01MH133334 & 2R01MH120080), and the Singapore National Research Foundation (NRF) Investigatorship (NRFI10-2024-0014). Any opinions, findings and conclusions or recommendations expressed in this material are those of the authors and do not reflect the views of the funders.

Statement of Ethics

Ethical approval was obtained by the National Healthcare group Domain Specific Review Board (DSRB 2023/000397). Written informed consent was obtained from participants (or their parent/legal guardian/next of kin) to participate in the study

Competing Interests

PCT declares that he has a non-remunerative patent for using brain imaging to select personalized targets for brain stimulation. BTTY and PCT are clinical advisors to a startup B1Neuro commercializing fMRI targeting software. RK, XWT, AX, SS, BTTY might financially

benefit from a pending patent covering the targeting algorithm used in the current study filed by the National University of Singapore (NUS). RK, LQRO, and BTTY hold shares in B1Neuro, which may license the patent from NUS. All other authors report no biomedical financial interests or potential conflicts of interest.

References

Afyouni, S., Smith, S.M., and Nichols, T.E. (2019). Effective degrees of freedom of the Pearson's correlation coefficient under autocorrelation. NeuroImage *199*, 609–625.

Beam, W., Borckardt, J.J., Reeves, S.T., and George, M.S. (2009). An efficient and accurate new method for locating the F3 position for prefrontal TMS applications. Brain Stimul *2*, 50–54.

Bergmann, T.O., Karabanov, A., Hartwigsen, G., Thielscher, A., and Siebner, H.R. (2016). Combining non-invasive transcranial brain stimulation with neuroimaging and electrophysiology: Current approaches and future perspectives. Neuroimage *140*, 4–19.

Blumberger, D.M., Vila-Rodriguez, F., Thorpe, K.E., Feffer, K., Noda, Y., Giacobbe, P., Knyahnytska, Y., Kennedy, S.H., Lam, R.W., Daskalakis, Z.J., et al. (2018). Effectiveness of theta burst versus high-frequency repetitive transcranial magnetic stimulation in patients with depression (THREE-D): a randomised non-inferiority trial. The Lancet *391*, 1683–1692.

Briggs, A. (1999). Handling uncertainty in economic evaluation. BMJ *319*, 120.

Briggs, A., Sculpher, M., and Claxton, K. (2006). Decision Modelling for Health Economic Evaluation (OUP Oxford).

Briley, P.M., Webster, L., Boutry, C., Oh, H., Auer, D.P., Liddle, P.F., and Morriss, R. (2024). Magnetic resonance imaging connectivity features associated with response to transcranial magnetic stimulation in major depressive disorder. Psychiatry Res Neuroimaging *342*, 111846.

Cash, R.F.H., Cocchi, L., Lv, J., Wu, Y., Fitzgerald, P.B., and Zalesky, A. (2021). Personalized connectivity-guided DLPFC-TMS for depression: Advancing computational feasibility, precision and reproducibility. Hum Brain Mapp *42*, 4155–4172.

Chodavadia, P., Teo, I., Poremski, D., Fung, D.S.S., and Finkelstein, E.A. (2023). Prevalence and economic burden of depression and anxiety symptoms among Singaporean adults: results from a 2022 web panel. BMC Psychiatry *23*, 104.

Chu, H.-T., Cheng, C.-M., Liang, C.-S., Chang, W.-H., Juan, C.-H., Huang, Y.-Z., Jeng, J.-S., Bai, Y.-M., Tsai, S.-J., Chen, M.-H., et al. (2021). Efficacy and tolerability of theta-burst stimulation for major depression: A systematic review and meta-analysis. Prog Neuropsychopharmacol Biol Psychiatry *106*, 110168.

Cole, E.J., Stimpson, K.H., Bentzley, B.S., Gulser, M., Cherian, K., Tischler, C., Nejad, R., Pankow, H., Choi, E., Aaron, H., et al. (2020). Stanford Accelerated Intelligent Neuromodulation Therapy for Treatment-Resistant Depression. AJP *177*, 716–726.

Cole, E.J., Phillips, A.L., Bentzley, B.S., Stimpson, K.H., Nejad, R., Barmak, F., Veerapal, C., Khan, N., Cherian, K., Felber, E., et al. (2022). Stanford Neuromodulation Therapy (SNT): A Double-Blind Randomized Controlled Trial. AJP *179*, 132–141.

Conway, C.R., George, M.S., and Sackeim, H.A. (2017). Toward an Evidence-Based, Operational Definition of Treatment-Resistant Depression: When Enough Is Enough. JAMA Psychiatry *74*, 9–10.

Dannhauer, M., Gomez, L.J., Robins, P.L., Wang, D., Hasan, N.I., Thielscher, A., Siebner, H.R., Fan, Y., and Deng, Z.-D. (2024). Electric Field Modeling in Personalizing Transcranial Magnetic Stimulation Interventions. Biol Psychiatry *95*, 494–501.

Deng, Z.-D., Robins, P.L., Dannhauer, M., Haugen, L.M., Port, J.D., and Croarkin, P.E. (2023). Optimizing TMS Coil Placement Approaches for Targeting the Dorsolateral Prefrontal Cortex in Depressed Adolescents: An Electric Field Modeling Study. Biomedicines *11*, 2320.

Drummond, M.F., Sculpher, M.J., Claxton, K., Stoddart, G.L., and Torrance, G.W. (2015). Methods for the Economic Evaluation of Health Care Programmes (Oxford University Press).

Elbau, I.G., Lynch, C.J., Downar, J., Vila-Rodriguez, F., Power, J.D., Solomonov, N., Daskalakis, Z.J., Blumberger, D.M., and Liston, C. (2023). Functional Connectivity Mapping for rTMS Target Selection in Depression. AJP *180*, 230–240.

Endicott, J., Nee, J., Harrison, W., and Blumenthal, R. (1993). Quality of Life Enjoyment and Satisfaction Questionnaire: a new measure. Psychopharmacology Bulletin *29*, 321–326.

Eshel, N., Keller, C.J., Wu, W., Jiang, J., Mills-Finnerty, C., Huemer, J., Wright, R., Fonzo, G.A., Ichikawa, N., Carreon, D., et al. (2020). Global connectivity and local excitability changes underlie antidepressant effects of repetitive transcranial magnetic stimulation. Neuropsychopharmacol. *45*, 1018–1025.

Fischl, B. (2012). FreeSurfer. Neuroimage *62*, 774–781.

Fitzgibbon, K.P., Plett, D., Chan, B.C.F., Hancock-Howard, R., Coyte, P.C., and Blumberger, D.M. (2020). Cost-Utility Analysis of Electroconvulsive Therapy and Repetitive Transcranial Magnetic Stimulation for Treatment-Resistant Depression in Ontario. Can J Psychiatry *65*, 164–173.

Fox, M.D., Buckner, R.L., White, M.P., Greicius, M.D., and Pascual-Leone, A. (2012). Efficacy of Transcranial Magnetic Stimulation Targets for Depression Is Related to Intrinsic Functional Connectivity with the Subgenual Cingulate. Biological Psychiatry *72*, 595–603.

Fox, M.D., Corbetta, M., Snyder, A.Z., Vincent, J.L., and Raichle, M.E. (2006). Spontaneous neuronal activity distinguishes human dorsal and ventral attention systems. PNAS *103*, 10046–10051.

Fox, M.D., Liu, H., and Pascual-Leone, A. (2013). Identification of reproducible individualized targets for treatment of depression with TMS based on intrinsic connectivity. NeuroImage *66*, 151–160.

Ge, R., Humaira, A., Gregory, E., Alamian, G., MacMillan, E.L., Barlow, L., Todd, R., Nestor, S., Frangou, S., and Vila-Rodriguez, F. (2022). Predictive Value of Acute Neuroplastic Response

to rTMS in Treatment Outcome in Depression: A Concurrent TMS-fMRI Trial. Am J Psychiatry *179*, 500–508.

George, M.S., Taylor, J.J., and Short, E.B. (2013). The expanding evidence base for rTMS treatment of depression. Curr Opin Psychiatry *26*, 13–18.

Goodman, M.S., Trevizol, A.P., Konstantinou, G.N., Boivin-Lafleur, D., Brender, R., Downar, J., Kaster, T.S., Knyahnytska, Y., Vila-Rodriguez, F., and Voineskos, D. (2025). Extended course accelerated intermittent theta burst stimulation as a substitute for depressed patients needing electroconvulsive therapy. Neuropsychopharmacology *50*, 685–694.

Group, T.E. (1990). EuroQol-a new facility for the measurement of health-related quality of life. Health Policy *16*, 199–208.

Hearne, L.J., Webb, L., Cash, R., Robinson, C., Mosley, P.E., Ng, J., Thwaites, S.T., Issa, S., Miller, J., and Yan Tse, N. (2025). Clinical and Neurophysiological Effects of Robotically Delivered fMRI-Guided Personalized Transcranial Magnetic Stimulation Therapy for Depression. Psychotherapy and Psychosomatics.

Ho, R.C., Mak, K.-K., Chua, A.N., Ho, C.S., and Mak, A. (2013). The effect of severity of depressive disorder on economic burden in a university hospital in Singapore. Expert Review of Pharmacoeconomics & Outcomes Research *13*, 549–559.

Huang, Y.-Z., and Rothwell, J.C. (2004). The effect of short-duration bursts of high-frequency, low-intensity transcranial magnetic stimulation on the human motor cortex. Clin Neurophysiol *115*, 1069–1075.

Huerta, P.T., and Volpe, B.T. (2009). Transcranial magnetic stimulation, synaptic plasticity and network oscillations. J Neuroeng Rehabil *6*, 7.

Jin, J., Wang, Y., Liang, S., Fan, Q., Li, M., Zhang, L., Cao, Y., Wang, Z., Li, R., Liu, H., et al. (2025). Effects of individualized rTMS on functional connectivity related to the default mode network and frontal-parietal network in major depressive disorder: exploratory analysis of a randomized controlled trial. Neuroimage Clin *48*, 103902.

Johnston, K.M., Powell, L.C., Anderson, I.M., Szabo, S., and Cline, S. (2019). The burden of treatment-resistant depression: A systematic review of the economic and quality of life literature. J Affect Disord *242*, 195–210.

Kong, R., Xue, A., Ooi, L.Q.R., Asplund, C., Tan, X.W., Goh, S.E., Lee, J.J., Koh, J.Z.J., Tan, R.S.Y., Singh, H.K.G., et al. (2025). Network-based Near-Scalp Personalized Brain Stimulation Targets. 2025.05.15.654391.

Kong, R., Li, J., Orban, C., Sabuncu, M.R., Liu, H., Schaefer, A., Sun, N., Zuo, X.-N., Holmes, A.J., Eickhoff, S.B., et al. (2019). Spatial Topography of Individual-Specific Cortical Networks Predicts Human Cognition, Personality, and Emotion. Cereb. Cortex *29*, 2533–2551.

Kozel, F.A., George, M.S., and Simpson, K.N. (2004). Decision analysis of the cost-effectiveness of repetitive transcranial magnetic stimulation versus electroconvulsive therapy for treatment of nonpsychotic severe depression. CNS Spectr *9*, 476–482.

Li, B., Zhao, N., Tang, N., Friston, K.J., Zhai, W., Wu, D., Liu, J., Chen, Y., Min, Y., Qiao, Y., et al. (2024). Targeting suicidal ideation in major depressive disorder with MRI-navigated Stanford accelerated intelligent neuromodulation therapy. Transl Psychiatry *14*, 1–12.

Li, J., Bzdok, D., Chen, J., Tam, A., Ooi, L.Q.R., Holmes, A.J., Ge, T., Patil, K.R., Jabbi, M., and Eickhoff, S.B. (2022). Cross-ethnicity/race generalization failure of behavioral prediction from resting-state functional connectivity. Science Advances *8*, eabj1812.

Li, J., Kong, R., Liégeois, R., Orban, C., Tan, Y., Sun, N., Holmes, A.J., Sabuncu, M.R., Ge, T., and Yeo, B.T.T. (2019). Global signal regression strengthens association between resting-state functional connectivity and behavior. NeuroImage *196*, 126–141.

Liston, C., Chen, A.C., Zebley, B.D., Drysdale, A.T., Gordon, R., Leuchter, B., Voss, H.U., Casey, B.J., Etkin, A., and Dubin, M.J. (2014). Default mode network mechanisms of transcranial magnetic stimulation in depression. Biol Psychiatry *76*, 517–526.

Lueckel, M., Radetz, A., Hassan, U., Yuen, K., Mueller-Dahlhaus, F., Kalisch, R., and Bergmann, T.O. (2023). Functional connectivity- and E-field-optimized TMS targeting: method development and concurrent TMS-fMRI validation. Brain Stimulation: Basic, Translational, and Clinical Research in Neuromodulation *16*, 189.

Luehr, J.G., Fritz, E., Turner, M., Schupp, C., and Sackeim, H.A. (2024). Accelerated transcranial magnetic stimulation: A pilot study of safety and efficacy using a pragmatic protocol. Brain Stimulation: Basic, Translational, and Clinical Research in Neuromodulation *17*, 860–863.

Lynch, C.J., Elbau, I.G., Ng, T.H., Wolk, D., Zhu, S., Ayaz, A., Power, J.D., Zebley, B., Gunning, F.M., and Liston, C. (2022). Automated optimization of TMS coil placement for personalized functional network engagement. Neuron *110*, 3263-3277.e4.

Lynch, C.J., Elbau, I.G., Ng, T., Ayaz, A., Zhu, S., Wolk, D., Manfredi, N., Johnson, M., Chang, M., Chou, J., et al. (2024). Frontostriatal salience network expansion in individuals in depression. Nature *633*, 624–633.

McIntyre, R.S., Alsuwaidan, M., Baune, B.T., Berk, M., Demyttenaere, K., Goldberg, J.F., Gorwood, P., Ho, R., Kasper, S., Kennedy, S.H., et al. (2023). Treatment-resistant depression: definition, prevalence, detection, management, and investigational interventions. World Psychiatry *22*, 394–412.

Montgomery, S.A., and Åsberg, M. (1979). A new depression scale designed to be sensitive to change. The British Journal of Psychiatry *134*, 382–389.

Nasreddine, Z.S., Phillips, N.A., Bédirian, V., Charbonneau, S., Whitehead, V., Collin, I., Cummings, J.L., and Chertkow, H. (2005). The Montreal Cognitive Assessment, MoCA: a brief

screening tool for mild cognitive impairment. Journal of the American Geriatrics Society *53*, 695–699.

Oathes, D.J., Duprat, R.J.-P., Reber, J., Liang, X., Scully, M., Long, H., Deluisi, J.A., Sheline, Y.I., and Linn, K.A. (2023). Non-invasively targeting, probing and modulating a deep brain circuit for depression alleviation. Nat. Mental Health *1*, 1033–1042.

Ooi, L.Q.R., Orban, C., Zhang, S., Nichols, T.E., Tan, T.W.K., Kong, R., Marek, S., Dosenbach, N.U.F., Laumann, T.O., Gordon, E.M., et al. (2025). Longer scans boost prediction and cut costs in brain-wide association studies. Nature *644*, 731–740.

Persson, M., Fabri, V., Reijbrandt, A., Lexén, A., Eriksson, H., and Movahed Rad, P. (2025). The Scania Accelerated Intermittent Theta-burst Implementation Study (SATIS)–Lessons from an accelerated treatment protocol. PloS One *20*, e0316339.

Philip, N.S., Barredo, J., van ’t Wout-Frank, M., Tyrka, A.R., Price, L.H., and Carpenter, L.L. (2018). Network Mechanisms of Clinical Response to Transcranial Magnetic Stimulation in Posttraumatic Stress Disorder and Major Depressive Disorder. Biol Psychiatry *83*, 263–272.

Ramos, M.R.F., Goerigk, S., da Silva, V.A., Cavendish, B.A., Pinto, B.S., Papa, C.H.G., Resende, J.V., Klein, I., Carneiro, A.M., and de Sousa, J.P. (2025). Accelerated Theta-Burst Stimulation for Treatment-Resistant Depression: A Randomized Clinical Trial. JAMA Psychiatry.

Ren, J., Su, W., Zhou, Y., Han, K., Pan, R., Duan, X., Liu, J., Lu, H., Zhang, P., Zhang, W., et al. (2025). Efficacy and safety of high-dose and personalized TBS on post-stroke cognitive impairment: A randomized controlled trial. Brain Stimulation *18*, 249–258.

Rush, A.J., Trivedi, M.H., Wisniewski, S.R., Nierenberg, A.A., Stewart, J.W., Warden, D., Niederehe, G., Thase, M.E., Lavori, P.W., Lebowitz, B.D., et al. (2006). Acute and longer-term outcomes in depressed outpatients requiring one or several treatment steps: a STAR*D report. Am J Psychiatry *163*, 1905–1917.

Rush, A.J., Trivedi, M.H., Ibrahim, H.M., Carmody, T.J., Arnow, B., Klein, D.N., Markowitz, J.C., Ninan, P.T., Kornstein, S., and Manber, R. (2003). The 16-Item Quick Inventory of Depressive Symptomatology (QIDS), clinician rating (QIDS-C), and self-report (QIDS-SR): a psychometric evaluation in patients with chronic major depression. Biological Psychiatry *54*, 573–583.

Sackeim, H.A., Haskett, R.F., Mulsant, B.H., Thase, M.E., Mann, J.J., Pettinati, H.M., Greenberg, R.M., Crowe, R.R., Cooper, T.B., and Prudic, J. (2001). Continuation pharmacotherapy in the prevention of relapse following electroconvulsive therapy: a randomized controlled trial. JAMA *285*, 1299–1307.

Schaefer, A., Kong, R., Gordon, E.M., Laumann, T.O., Zuo, X.-N., Holmes, A.J., Eickhoff, S.B., and Yeo, B.T.T. (2018). Local-Global Parcellation of the Human Cerebral Cortex from Intrinsic Functional Connectivity MRI. Cerebral Cortex *28*, 3095–3114.

Sforzini, L., Worrell, C., Kose, M., Anderson, I.M., Aouizerate, B., Arolt, V., Bauer, M., Baune, B.T., Blier, P., Cleare, A.J., et al. (2022). A Delphi-method-based consensus guideline for definition of treatment-resistant depression for clinical trials. Mol Psychiatry *27*, 1286–1299.

Sheehan, D.V., Harnett-Sheehan, K., and Raj, B. (1996). The measurement of disability. International Clinical Psychopharmacology *11*, 89–95.

Siddiqi, S.H., Weigand, A., Pascual-Leone, A., and Fox, M.D. (2021). Identification of Personalized Transcranial Magnetic Stimulation Targets Based on Subgenual Cingulate Connectivity: An Independent Replication. Biol Psychiatry *90*, e55–e56.

Siddiqi, S.H., Kandala, S., Hacker, C.D., Trapp, N.T., Leuthardt, E.C., Carter, A.R., and Brody, D.L. (2023). Individualized precision targeting of dorsal attention and default mode networks with rTMS in traumatic brain injury-associated depression. Sci Rep *13*, 4052.

Sonnenberg, F.A., and Beck, J.R. (1993). Markov models in medical decision making: a practical guide. Med Decis Making *13*, 322–338.

Spitzer, R.L., Kroenke, K., Williams, J.B., and Löwe, B. (2006). A brief measure for assessing generalized anxiety disorder: the GAD-7. Archives of Internal Medicine *166*, 1092–1097.

Stöhrmann, P., Godbersen, G.M., Reed, M.B., Unterholzner, J., Klöbl, M., Baldinger-Melich, P., Vanicek, T., Hahn, A., Lanzenberger, R., Kasper, S., et al. (2023). Effects of bilateral sequential theta-burst stimulation on functional connectivity in treatment-resistant depression: First results. Journal of Affective Disorders *324*, 660–669.

Stokes, M.G., Chambers, C.D., Gould, I.C., Henderson, T.R., Janko, N.E., Allen, N.B., and Mattingley, J.B. (2005). Simple Metric For Scaling Motor Threshold Based on Scalp-Cortex Distance: Application to Studies Using Transcranial Magnetic Stimulation. Journal of Neurophysiology *94*, 4520–4527.

Sun, W., Billot, A., Du, J., Wei, X., Lemley, R.A., Daneshzand, M., Nummenmaa, A., Buckner, R.L., and Eldaief, M.C. (2024). Precision Network Modeling of Transcranial Magnetic Stimulation Across Individuals Suggests Therapeutic Targets and Potential for Improvement. medRxiv 2024.08.15.24311994.

Teng, M., Khoo, A.L., Zhao, Y.J., Abdin, E., Mok, Y.M., Lim, B.P., and Tor, P.C. (2021). Neurostimulation therapies in major depressive disorder: A decision-analytic model. Early Interv Psychiatry *15*, 1531–1541.

Thase, M.E., and Rush, A.J. (1997). When at first you don't succeed: sequential strategies for antidepressant nonresponders. J Clin Psychiatry *58 Suppl 13*, 23–29.

Thielscher, A., Antunes, A., and Saturnino, G.B. (2015). Field modeling for transcranial magnetic stimulation: A useful tool to understand the physiological effects of TMS? Annu Int Conf IEEE Eng Med Biol Soc *2015*, 222–225.

Tor, P.C., Amir, N., Fam, J., Ho, R., Ittasakul, P., Maramis, M.M., Ponio, B., Purnama, D.A., Rattanasumawong, W., and Rondain, E. (2022). A Southeast Asia consensus on the definition and management of treatment-resistant depression. Neuropsychiatric Disease and Treatment 2747–2757.

Weigand, A., Horn, A., Caballero, R., Cooke, D., Stern, A.P., Taylor, S.F., Press, D., Pascual-Leone, A., and Fox, M.D. (2018). Prospective Validation That Subgenual Connectivity Predicts Antidepressant Efficacy of Transcranial Magnetic Stimulation Sites. Biological Psychiatry *84*, 28–37.

Weinstein, M.C., Siegel, J.E., Gold, M.R., Kamlet, M.S., and Russell, L.B. (1996). Recommendations of the Panel on Cost-effectiveness in Health and Medicine. JAMA *276*, 1253–1258.

Weis, S., Patil, K.R., Hoffstaedter, F., Nostro, A., Yeo, B.T.T., and Eickhoff, S.B. (2020). Sex Classification by Resting State Brain Connectivity. Cerebral Cortex *30*, 824–835.

Williams, N.R., Sudheimer, K.D., Bentzley, B.S., Pannu, J., Stimpson, K.H., Duvio, D., Cherian, K., Hawkins, J., Scherrer, K.H., and Vyssoki, B. (2018). High-dose spaced theta-burst TMS as a rapid-acting antidepressant in highly refractory depression. Brain *141*, e18–e18.

Ye, S.J., Lu, L., Phu, H.H., Tan, X.W., and Tor, P.C. (2024). Repetitive transcranial magnetic stimulation for major depression and obsessive-compulsive disorders in Singapore. Annals of the Academy of Medicine, Singapore *53*, 471–480.

Zemplényi, A., Józwiak-Hagymásy, J., Kovács, S., Erdősi, D., Boncz, I., Tényi, T., Osváth, P., and Voros, V. (2022). Repetitive transcranial magnetic stimulation may be a cost-effective alternative to antidepressant therapy after two treatment failures in patients with major depressive disorder. BMC Psychiatry *22*, 437.

Zhang, B.B., Lin, T.T. ze, Qin, P.P., Jin, M., Xia, A.W., Kan, R.L. di, Zhu, F.F., and Kranz, G. (2025). Rethinking intensity: Repetitive transcranial magnetic stimulation across ethnic populations. medRxiv 2025.02. 22.25322728.

Zhao, H., Jiang, C., Zhao, M., Ye, Y., Yu, L., Li, Y., Luan, H., Zhang, S., Xu, P., and Chen, X. (2024). Comparisons of accelerated continuous and intermittent theta burst stimulation for treatment-resistant depression and suicidal Ideation. Biological Psychiatry *96*, 26–33.

Zhao, Y.J., Tor, P.C., Khoo, A.L., Teng, M., Lim, B.P., and Mok, Y.M. (2018). Cost-Effectiveness Modeling of Repetitive Transcranial Magnetic Stimulation Compared to Electroconvulsive Therapy for Treatment-Resistant Depression in Singapore. Neuromodulation: Technology at the Neural Interface *21*, 376–382.

Supplementary Material

This supplemental material is divided into Supplemental Methods and Supplemental Results to complement the Methods and Results sections in the main text, respectively.

Supplementary Methods

Clinical assessments

Participants completed a comprehensive battery of clinician-rated and self-reported measures, including the Montgomery–Åsberg Depression Rating Scale (MADRS) score (Montgomery and Åsberg, 1979), Quick Inventory of Depressive Symptomatology (QIDS-SR16; Rush et al., 2003), Generalized Anxiety Disorder-7 (GAD-7; Spitzer et al., 2006), Montreal Cognitive Assessment (MoCA; Nasreddine et al., 2005), Sheehan Disability Scale (SDS; Sheehan et al., 1996), EuroQol-5D (EQ-5D; Group, 1990), and the Quality of Life Enjoyment and Satisfaction Questionnaire (Q-LES-Q-SF; Endicott et al., 1993).

Assessments were conducted at baseline, post-treatment, 1-month, and 3-month follow-ups by trained raters. Side effects were systematically recorded throughout the study. In addition, daily QIDS-SR16 and GAD-7 scores were collected at the end of each treatment day to capture short-term symptom changes over the course of treatment.

Clinical outcome analysis

All efficacy analyses followed an intent-to-treat principle. Primary outcome was treatment response, defined as ≥50% reduction in MADRS scores from baseline in any post-treatment assessment conducted within four weeks of completing the acute TAO-TMS course. Secondary outcomes included remission (MADRS <11), QIDS-SR16, GAD-7, MoCA, SDS, EQ-5D, and Q-LES-Q-SF. Response and remission rates were also evaluated at each specific post-treatment timepoint (immediately post-treatment, 1-month, and 3-month follow-up).

All statistical analysis were conducted using SPSS, version 27 (IBM, Armonk, N.Y.). Treatment outcomes across different timepoints were compared using paired t-tests. Repeated measures ANOVA were conducted to examine the effect of treatment on outcomes across time. Assumptions of sphericity were tested using Mauchly's test. When the assumption was

violated, the Greenhouse-Geisser correction was applied. Effect sizes were reported using partial eta squared (η^2) or Cohen's d. Significance was set at p=0.05.

MRI acquisition

All MRI scans were acquired at the Centre for Translational Magnetic Resonance Research (TMR), National University of Singapore, on a 3T Siemens Prisma Fit scanner. Each participant underwent a T1-weighted structural scan and two 10-minute resting-state fMRI (rs-fMRI) runs prior to treatment. The structural data were obtained with T1w MPRAGE sequence using the following acquisition parameters: TR = 2200 ms; TE = 2.45 ms; FOV = 256 × 232 mm; voxel resolution = 1.0 × 1.0 × 1.0-mm voxels. The rs-fMRI data were obtained with the following acquisition parameters: TR = 1000 ms; TE = 12, 29.75, 47.5 ms; multiband factor 4; flip angle = 50°; FOV = 240 × 240 mm; voxel resolution = 3.0 × 3.0 × 3.0-mm voxels. During the 10-minute rs-fMRI scans, participants were instructed to keep their eyes open, maintain fixation on a central cross, let their minds wander naturally, and avoid repetitive thoughts. The scalp-based BeamF3 (Beam et al., 2009) stimulation location was also identified and marked on the scalp using a vitamin E capsule. Participants completed a second MRI session on average 5.0 ± 1.9 days after treatment, consisting of one T1-weighted structural scan and two resting-state fMRI runs acquired using the same imaging protocol.

fMRI preprocessing

T1 MRI was processed using FreeSurfer (Fischl, 2012). Resting-state fMRI data were preprocessed using the Computational Brain Imaging Group (CBIG) fMRI preprocessing pipeline (Kong et al., 2019; Li et al., 2019; Ooi et al., 2025). Preprocessing included the following steps. (1) Removal of the first 4 frames; (2) Slice time correction; (3) Motion correction and outlier detection: frames with FD > 0.2 mm or DVARS > 75 were flagged as censored frames. 1 frame before and 2 frames after these volumes were flagged as censored frames. Uncensored segments of data lasting fewer than five contiguous frames were also labeled as censored frames. Runs with over half of the frames censored were removed; After censoring, there might be less than 10 min of data for a particular run, but in the result section, we will still refer to uncensored frames as a 10-min run. (4) Correcting for susceptibility-induced spatial distortion; (5) Multi-echo denoising (DuPre et al., 2021); (6)

Alignment with structural image using boundary-based registration (Greve and Fischl, 2009); (7) Global, white matter and ventricular signals, 6 motion parameters, and their temporal derivatives were regressed from the functional data. Regression coefficients were estimated from uncensored data; (8) Censored frames were interpolated with the Lomb-Scargle periodogram (Power et al., 2014); (9) Bandpass filtering (0.009 Hz – 0.08 Hz) was applied to the data; (10) The data was then projected onto FreeSurfer fsaverage6 surface space and smoothed using a 6 mm full-width half maximum kernel; (11) Lastly, preprocessed data in native fMRI volumetric space was smoothed using a 4mm full-width half maximum kernel. Alignment between T1 and MNI152 was also computed using ANTs registration (Avants et al., 2011).

Health Economic Evaluation

A decision-analytical model was used to estimate the cost-effectiveness of TAO-TMS (Tree-based Algorithm for Optimized Transcranial Magnetic Stimulation) in comparison to electroconvulsive therapy (ECT). We employed a hybrid approach combining a decision tree and a Markov model to represent treatment responses and transitions between different health states following treatment. The model commenced with a decision tree that simulates treatment responses, which were categorized as follows: response (50% reduction in MADRS), partial response (25% to 50% reduction in MADRS), and no response (less than 25% reduction in MADRS). After classifying patients based on these treatment responses, we utilized a Markov model to simulate changes in health states, defined as remission (MADRS less than 11), partial relapse (MADRS between 11 and 20), and relapse (MADRS above 20). The Markov health states operated on a cycle length of one month, allowing patients to transition from one health state to another at each cycle until the time horizon was reached.

Clinical, cost, and EQ-5D data collected from the study informed the inputs for TAO-TMS. Due to the absence of data for ECT, clinical data for ECT were sourced from the literature. The primary outcomes from the cost-effectiveness analysis (CEA) model included costs, quality-adjusted life years (QALY) gained, and the incremental cost-effectiveness ratio (ICER). We established a willingness-to-pay (WTP) threshold of S$100,000 (US$77,519).

Base-case analyses were conducted with a one-year time horizon from two distinct perspectives: the health system and society. From the health system perspective, we included direct costs associated with health services utilized for treatment, while the societal

perspective encompassed indirect costs such as productivity loss due to absenteeism and income loss.

One-way and probabilistic sensitivity analyses were performed on the base-case analyses to evaluate the impact of extreme values in input parameters on the results and to assess the robustness of variations in individual input parameters across different WTP thresholds. Additionally, we conducted scenario analyses with time horizons of three months and six months, as well as a conservative scenario involving two health states.

All costs were analyzed in Singapore Dollars (SGD) for the year 2025 and results are presented in US Dollars (USD) using exchange rate of 1 USD = 1.29 SGD, and no discounting was applied to costs and QALY since the time horizons were less than one year. Data cleaning and analyses for health economic evaluation (HEE) were performed using RStudio Desktop Pro, version 2024.04.1 (Posit Software, PBC, Boston, MA), while modelling was conducted in TreeAge Pro 2023, R2 (TreeAge Software, LLC, Williamstown, MA).

Supplementary Results

Cost-effectiveness analysis

A hybrid decision tree and Markov cohort model (Figure S1) was used to assess the costs and effectiveness of TAO-TMS and ECT, utilizing data collected from the study and relevant literature (Table S4). From the perspective of the health system, TAO-TMS demonstrated a cost reduction of US$9,523 compared to ECT, with costs amounting to US$33,708 for TAO-TMS versus US$43,231 for ECT. Additionally, TAO-TMS resulted in a higher QALY of 0.69, compared to 0.65 for ECT. When viewed from a societal perspective, the cost savings associated with TAO-TMS were even more pronounced, amounting to US$28,316 less than ECT. The combination of cost savings and the greater QALY associated with TAO-TMS positioned it as the preferred option over ECT from both health system and societal viewpoints (Table S5).

Tornado diagrams were employed to illustrate the outcomes of the one-way sensitivity analyses (Figure S8). Under the health system perspective, the cost of ECT treatment emerged as the most significant input parameter influencing the results. Specifically, if the cost of ECT treatment were to decrease to below US$280 USD (S$361), the ICER would exceed the WTP threshold, thereby altering the conclusion regarding the cost-effectiveness of

TAO-TMS. In contrast, from the societal perspective, none of the extreme values of the input parameters were found to affect the determination of TAO-TMS as a cost-effective option.

In the probabilistic sensitivity analyses, we conducted 10,000 iterations of Monte Carlo simulations, varying the input parameters simultaneously. The results were presented in cost-effectiveness acceptability curves (CEACs), which illustrate the probabilities of each intervention arm being cost-effective across a range of WTP thresholds. The CEACs (Figure 6) demonstrate that TAO-TMS was dominant across various WTP thresholds from both perspectives, suggesting that the base-case results were robust.

In scenarios involving shorter time horizons, the cost savings and QALY gains associated with TAO-TMS were diminished across all scenarios (Table S6). Nevertheless, despite the reduced benefits in terms of costs and QALY gains, TAO-TMS continued to be the dominant option when compared to ECT. In a conservative scenario that considered only two treatment responses and two Markov health states (Figure S9), TAO-TMS still demonstrated cost savings relative to ECT (Table S7). However, the QALY gains were found to be comparable between the two treatments, with ECT yielding 0.01 QALY gain compared to TAO-TMS. The ICER in this conservative scenario was calculated at US$684,300 (ECT versus TAO-TMS) for the health system perspective and US$163,800 (ECT versus TAO-TMS) for the societal perspective, both of which significantly exceed the WTP threshold, thereby confirming that TAO-TMS remained the cost-effective option.

Table S1. Patient socio-demographics, clinical characteristics, and TMS parameters.

Baseline Characteristics		Total Sample (N=21)	
		Mean	SD
Age (years)		35	12
		No.	%
Gender	Female	12	57
	Male	9	43
Diagnosis/comorbidities	Major depressive disorder	21	100
	Generalized anxiety disorder	12	57
	Post-traumatic stress disorder	6	29
	Personality disorder	6	29
	Feeding and eating disorder	5	24
	Autism spectrum disorder	3	14
	Bipolar disorder	1	5
	Attention-deficit/hyperactivity disorder	1	5
	Obsessive-compulsive disorder	1	5
	Gender dysphoria with affirmative surgery	1	5
	Breast and kidney cancer	1	5
	Hepatitis B	1	5
Duration of current depressive episode	Acute (≤12 months)	11	52
	Sub-acute	5	24
	Chronic (>24 months)	5	24
Number of previous depressive episodes	1 to 3	3	14
	>3	18	86
Antidepressants (AD)	NO	2	10
	YES	19	91
Antipsychotics	NO	8	38
	YES	13	62
Clozapine	NO	21	100
	YES	0	0
Lithium	NO	18	86
	YES	3	14
Benzodiazepine	NO	10	48
	YES	11	52
Anticonvulsants	NO	16	76
	YES	5	24
Stimulants	NO	21	100
	YES	0	0
Augmentation	NO	8	38

	YES	13	62
		Mean	SD
Number of failed AD trials		4.67	2.27
		Count	%
Past ECT treatment	NO	17	81
	YES	4	19
Past TMS treatment	NO	13	62
	YES	8	38
		Mean	SD
TMS Treatment Variables	Resting motor threshold (RMT)	60	12
	TMS dosage [a]	54	11
	COBOT deviation (mm)	1.83	0.67

[a] TMS dosage was set at 90% RMT with individualized depth correction.

Table S2. Clinical assessment scores of the intent-to-treat sample at the various respective timepoints of TAO-TMS [a]

Assessment scores								
	Baseline		Post-treatment		1-month FU		3-month FU	
	(Mean ± SD)	N	(Mean ± SD)	N	(Mean ± SD)	N	(Mean ± SD)	N
MADRS	28.33 ± 5.14		12.10 ± 5.56		18.06 ± 10.12		20.13 ± 7.71	
QIDS-SR16	20.67 ± 6.45		11.30 ± 6.61		14.44 ± 8.13		16.44 ± 8.33	
GAD-7	10.86 ± 5.26		6.90 ± 5.04		8.94 ± 5.58		10.38 ± 3.74	
Q-LES-Q-SF	39.00 ± 9.64		43.15 ± 9.29		42.44 ± 11.21		44.69 ± 11.38	
EQ-5D-3L utility score	0.39 ± 0.33		0.60 ± 0.28		0.51 ± 0.40		0.41 ± 0.45	
· Visual analogue scale	42.62 ± 16.50	21	59.65 ± 17.54	20	57.78 ± 24.09	18	49.69 ± 16.78	16
SDS total score	17.86 ± 6.46		14.30 ± 7.66		11.71 ± 9.48		13.63 ± 6.35	
· Days lost	3.61 ± 2.89		1.80 ± 2.46		1.33 ± 1.99		2.54 ± 2.99	
· Days underproductive	5.12 ± 2.20		2.92 ± 2.50		3.53 ± 2.90		3.23 ± 2.80	
MoCA	28.52 ± 1.47		28.00 ± 1.65		27.59 ± 2.32		28.73 ± 1.22	
MADRS-Q10	2.52 ± 1.33		1.25 ± 0.79		1.78 ± 1.67		2.25 ± 1.39	
	Rate (%)	N	Rate (%)	N	Rate (%)	N	Rate (%)	N
Response [a]	-	-	65	13	50	9	31.25	5
Remission [b]	-	-	30	6	27.78	5	6.25	1

Abbreviations: MADRS, Montgomery-Asberg Depression Rating Scale; QIDS-SR16, The Quick Inventory of Depressive Symptomatology (16-Item) (Self-Report); GAD-7, Generalized Anxiety Disorder-7 item; Q-LES-Q-SF, Quality of Life Enjoyment and Satisfaction Questionnaire-Short form; EQ-5D-3L, EuroQol 5-dimensional questionnaire with 3-levels; SDS, Sheehan Disability Scale; MoCA, the Montreal Cognitive Assessment; FU: follow-up

[a] Response was defined as a ≥50% reduction in total MADRS scores against baseline scores.

[b] Remission was defined as a total MADRS score of <11.

Table S3. Statistical analyses report for the comparisons of clinical assessments and sociodemographic factors.

Tests used	Comparators within groups	df	p value	Effect Size (Cohen's d)	lower 95% CI	upper 95% CI
Paired t test (MADRS)	Baseline vs Post-treatment	19	<0.001	2.176	12.755	19.745
	Baseline vs 1-month FU	17	<0.001	1.052	5.332	14.890
	Baseline vs 3-month FU	15	<0.001	1.284	4.644	11.231
	Post-treatment vs 1-month FU	17	0.014	-0.646	-10.816	-1.406
	Post-treatment vs 3-month FU	15	0.004	-0.856	-12.273	-2.852
	1-month FU vs 3-month FU	14	0.300	-0.278	-8.781	2.914
Paired t test (QIDS-SR16)	Baseline vs Post-treatment	19	<0.001	1.354	6.217	12.783
	Baseline vs 1-month FU	17	0.001	0.894	2.713	9.509
	Baseline vs 3-month FU	15	0.006	0.808	1.594	7.781
	Post-treatment vs 1-month FU	17	0.058	-0.479	-6.230	0.119
	Post-treatment vs 3-month FU	15	0.059	-0.511	-9.960	0.210
	1-month FU vs 3-month FU	14	0.345	-0.252	-7.240	2.706
Paired t test (GAD-7)	Baseline vs Post-treatment	19	<0.001	1.228	2.537	5.663
	Baseline vs 1-month FU	17	0.069	0.457	-0.147	3.480
	Baseline vs 3-month FU	15	0.232	0.311	-1.023	3.898
	Post-treatment vs 1-month FU	17	0.021	-0.600	-4.064	-0.381
	Post-treatment vs 3-month FU	15	0.016	-0.675	-4.250	-0.500
	1-month FU vs 3-month FU	14	0.690	-0.105	-3.340	2.274
		Z score	p value	Effect Size (r)		
Wilcoxon Signed-Rank test (MADRS)	Baseline vs Post-treatment	-3.922	<0.001	-0.620		
	Baseline vs 1-month FU	-3.104	0.002	-0.517		
	Baseline vs 3-month FU	-3.468	0.001	-0.613		
Wilcoxon Signed-Rank test (QIDS-SR16)	Baseline vs Post-treatment	-3.784	<0.001	-0.598		
	Baseline vs 1-month FU	-2.821	0.005	-0.470		
	Baseline vs 3-month FU	-2.593	0.010	-0.458		
Wilcoxon Signed-Rank test (GAD-7)	Baseline vs Post-treatment	-3.774	<0.001	-0.597		
	Baseline vs 1-month FU	-1.713	0.087	-0.286		
	Baseline vs 3-month FU	-0.935	0.350	-0.165		
	Comparators across groups	df	p value	Effect Size (partial η^2)		
Repeated measures ANOVA (MADRS)	Within-subjects Effects	3	<0.001	0.564		
	Between-subjects Effects	14	0.110	0.352		
Repeated measures ANOVA (QIDS-SR16)	Within-subjects Effects	3	<0.001	0.367		
	Between-subjects Effects	14	<0.001	0.548		
Repeated measures ANOVA (GAD-7)	Within-subjects Effects	3	0.010	0.234		
	Between-subjects Effects	14	<0.001	0.744		

		df	p value	Effect Size (φ)		
Pearson's Chi Square test	Gender	1	0.888	0.032		
	MDD diagnosis only (no comorbidities)	1	0.948	0.015		
	MDD and GAD (no other comorbidities)	1	0.444	0.171		
	Employment status	1	0.160	-0.314		

Abbreviations: MADRS, Montgomery-Asberg Depression Rating Scale; QIDS-SR16, The Quick Inventory of Depressive Symptomatology (16-Item) (Self-Report); GAD-7, Generalized Anxiety Disorder-7 item; FU: follow-up; MDD, Major Depressive Disorder.

Table S4. Input parameters for the health economic evaluation comparing TAO-TMS and ECT.

Parameters	Base value (SD)	Low	High	Distribution	Data sources
Treatment costs (SGD)					
fMRI acquisition	1,158	365	5,000	Gamma	ACE resource sheet, hospital database, expert's opinion
fMRI analysis	2,000	1,000	3,000	Gamma	Expert's opinion
aTMS	150	130	200	Gamma	Expert's opinion, hospital database
ECT	1,700	300	2,600	Gamma	MOH, hospital database
Health state direct costs (SGD)					
Remission					
Outpatient visits	333 (232)	-	-	Gamma	Hospital database, study data
Adverse event	8,988 (8,988)	-	-	Gamma	Hospital database, study data
Laboratory tests	15.6 (15.6)	-	-	Gamma	Hospital database, study data
Medications	965 (2,034)	-	-	Gamma	Hospital database, study data
Partial Relapse					
Outpatient visits	325 (223)	-	-	Gamma	Hospital database, study data
Adverse event	10,289.5 (650.75)	-	-	Gamma	Hospital database, study data
Laboratory tests	45.3 (21.2)	-	-	Gamma	Hospital database, study data
Medications	1,254 (3,416)	-	-	Gamma	Hospital database, study data
Relapse					
Outpatient visits	488 (321)	-	-	Gamma	Hospital database, study data
Adverse event	11,591 (8,489)	-	-	Gamma	Hospital database, study data
Laboratory tests	88.2 (42.1)	-	-	Gamma	Hospital database, study data
Medications	455 (479)	-	-	Gamma	Hospital database, study data
Indirect costs (SGD)					
Transport to outpatient visits	8.13 (6.78)	-	-		
Transport to adverse event episode	16 (16)	-	-		
Transport to laboratory test	3.2 (3.2)	-	-		
Median salary	5,500 (5,500)	-	-		
Utility scores					
Treatment resistant depression	0.524 (0.27)	-	-	Beta	Study data
Response	0.747 (0.184)	-	-	Beta	Study data
Partial response	0.66 (0.22)	-	-	Beta	Study data
Remission	0.684 (0.2)	-	-	Beta	Study data
Partial relapse	0.641 (0.197)	-	-	Beta	Study data
Relapse	0.54 (0.152)	-	-	Beta	Study data
Probabilities					
Response in TAO-TMS	0.65 (0.325)	-	-	-	Study data

Partial response in TAO-TMS	0.35 (0.175)	-	-	-	Study data
Response in ECT	0.666 (0.333)	-	-	-	Fitzgibbon et al., 2020
Initial probability of remission in TAO-TMS	0.6	-	-	-	Study data
Initial probability of partial relapse in TAO-TMS	0.3	-	-	-	Study data
Initial probability of remission in ECT	0.509	-	-	-	Fitzgibbon et al., 2020
Initial probability of partial relapse in ECT	0	-	-	-	No data
Remission to partial in TAO-TMS					
Month 1 to 3	0.4	-	-	-	Study data
Month 3 onwards	0.4	-	-	-	Study data
Remission to relapse in TAO-TMS					
Month 1 to 3	0.2	-	-	-	Study data
Month 3 onwards	0.4	-	-	-	Study data
Partial relapse to remission					
Month 1 to 3	0.25	-	-	-	Study data
Month 3 onwards	0	-	-	-	Study data
Partial relapse to relapse					
Month 1 to 3	0.33	-	-	-	Study data
Month 3 onwards	0.33	-	-	-	Study data
Relapse to remission					
Month 1 to 3	0	-	-	-	Study data
Month 3 onwards	0	-	-	-	Study data
Relapse to partial relapse					
Month 1 to 3	0	-	-	-	Study data
Month 3 onwards	0.25	-	-	-	Study data
Remission to partial in ECT	0	-	-	-	
Remission to relapse in ECT	0.34	-	-	-	Zhao et al., 2018
Partial to remission in ECT	0.7	-	-	-	Zhao et al., 2018
Partial to relapse in ECT	0.3	-	-	-	Zhao et al., 2018
Relapse to remission in ECT	0	-	-	-	No data
Relapse to partial in ECT	0	-	-	-	No data

SD: Standard deviation

All costs were expressed in 2025 Singapore Dollars (SGD).

Table S5. Base-case cost-effectiveness results from health system and societal perspectives.

Perspectives	Strategies	Costs (SGD)	Incremental cost (SGD)	QALY	Incremental QALY	ICER (SGD/QALY)
Health system	TAO-TMS	43,483	-	0.69	-	-
	ECT	55,767	12,284	0.65	-0.04	-325,186
Societal	TAO-TMS	109,582	-	0.69	-	-
	ECT	146,109	36,527	0.65	-0.04	-966,949

Perspectives	Strategies	Costs (USD)	Incremental cost (USD)	QALY	Incremental QALY	ICER (USD/QALY)
Health system	TAO-TMS	33,708	-	0.69	-	-
	ECT	43,231	9,523	0.65	-0.04	-252,083
Societal	TAO-TMS	84,947	-	0.69	-	-
	ECT	113,263	28,316	0.65	-0.04	-749,573

TAO-TMS: Tree-based Algorithm for Optimized Transcranial Magnetic Stimulation, ECT: electroconvulsive therapy; QALY: quality-adjusted life-year; ICER: incremental cost-effectiveness ratio. All costs were analyzed in 2025 Singapore Dollars (SGD) and converted to US Dollars (USD) with currency conversion of 1 USD = 1.29 SGD.

Table S6. Scenario analyses examining cost-effectiveness of TAO-TMS over shorter time horizons (3-month and 6-month models).

Scenarios	Strategies	Costs (SGD)	Incremental cost (SGD)	QALY	Incremental QALY	ICER (SGD/QALY)
Health system						
Time horizon of 3 months	TAO-TMS	18,550	-	0.26	-	-
	ECT	28,777	12,807	0.25	-0.01	-1,280,712
Time horizon of 6 months	TAO-TMS	26,897	-	0.4	-	-
	ECT	37,662	10,765	0.38	-0.02	-538,253
Societal						
Time horizon of 3 months	TAO-TMS	32,651	-	0.26	-	-
	ECT	47,725	15,074	0.25	-0.01	-1,507,365
Time horizon of 6 months	TAO-TMS	58,720	-	0.4	-	-
	ECT	79,487	20,768	0.38	-0.02	-1,038,386

Scenarios	Strategies	Costs (USD)	Incremental cost (USD)	QALY	Incremental QALY	ICER (USD/QALY)
Health system						
Time horizon of 3 months	TAO-TMS	14,380	-	0.26	-	-
	ECT	22,308	9,928	0.25	-0.01	-992,800
Time horizon of 6 months	TAO-TMS	20,850	-	0.40	-	-
	ECT	29,195	8,345	0.38	-0.02	-417,250
Societal						
Time horizon of 3 months	TAO-TMS	25,311	-	0.26	-	-
	ECT	36,996	11,685	0.25	-0.01	-1,168,500
Time horizon of 6 months	TAO-TMS	45,519	-	0.40	-	-
	ECT	61,618	16,099	0.38	-0.02	-804,950

TAO-TMS: Tree-based Algorithm for Optimized Transcranial Magnetic Stimulation, ECT: electroconvulsive therapy; QALY: quality-adjusted life-year; ICER: incremental cost-effectiveness ratio. All costs were analyzed in 2025 Singapore Dollars (SGD) and converted to US Dollars (USD) with currency conversion of 1 USD = 1.29 SGD.

Table S7. Scenario analyses using conservative two-state Markov model structures.

Perspectives	Strategies	Costs (SGD)	Incremental cost (SGD)	QALY	Incremental QALY	ICER (SGD/QALY)
Health system	TAO-TMS	45,122	-	0.72	-	-
	ECT	53,949	8,827	0.73	0.01	882,747
Societal	TAO-TMS	122,038	-	0.72	-	-
	ECT	124,151	2,113	0.73	0.01	211,302

Perspectives	Strategies	Costs (USD)	Incremental cost (USD)	QALY	Incremental QALY	ICER (USD/QALY)
Health system	TAO-TMS	34,978	-	0.72	-	-
	ECT	41,821	6,843	0.73	0.01	684,300
Societal	TAO-TMS	94,603	-	0.72	-	-
	ECT	96,241	1,638	0.73	0.01	163,800

TAO-TMS: Tree-based Algorithm for Optimized Transcranial Magnetic Stimulation, ECT: electroconvulsive therapy; QALY: quality-adjusted life-year; ICER: incremental cost-effectiveness ratio. All costs were analyzed in 2025 Singapore Dollars (SGD) and converted to US Dollars (USD) with currency conversion of 1 USD = 1.29 SGD.

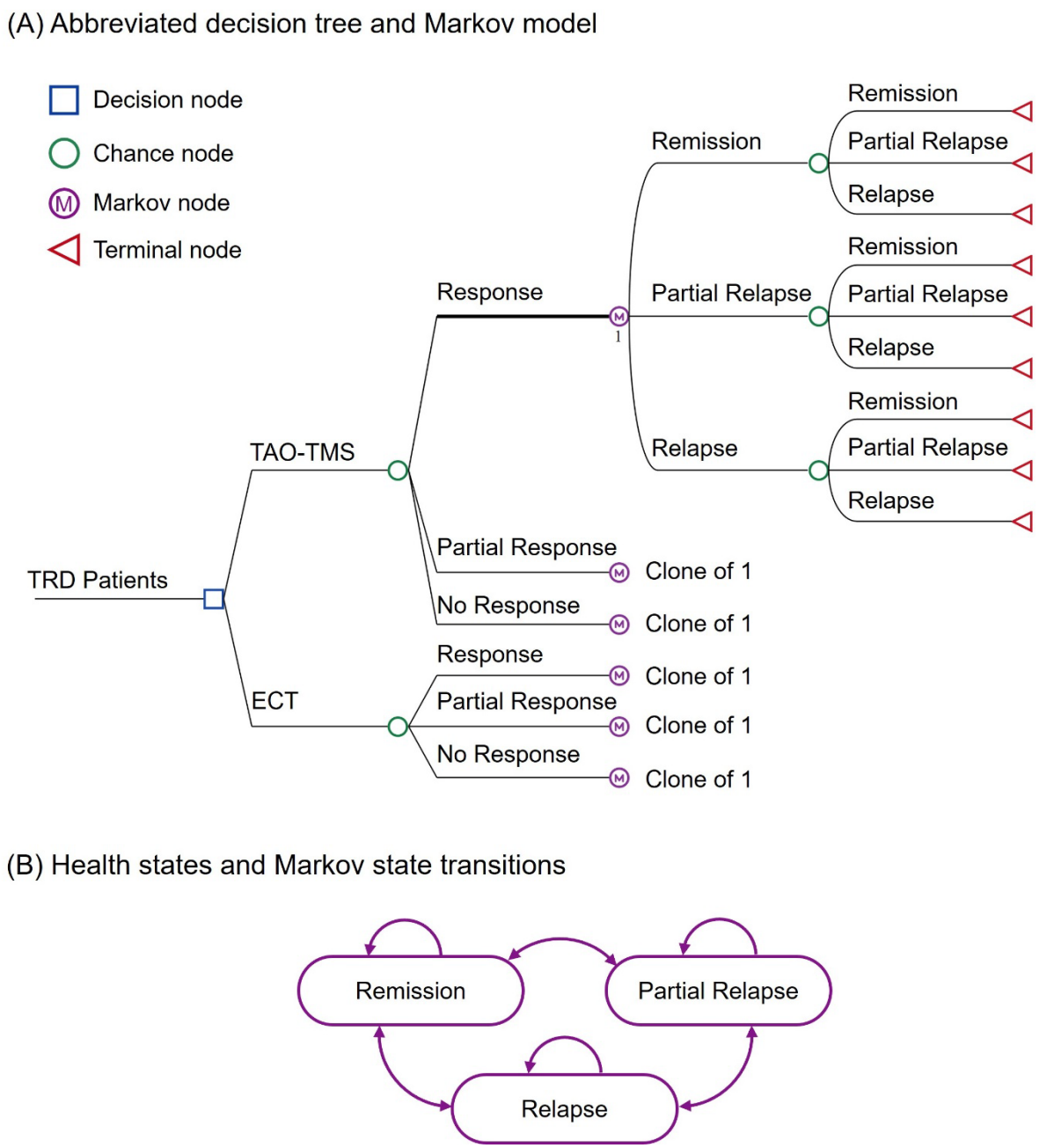

Figure S1. Decision analytical model comparing TAO-TMS and ECT. (A) Abbreviated decision tree and Markov model representing the clinical pathways for patients receiving TAO-TMS or ECT. Initial treatment decisions from the decision tree fed into the Markov model for long-term simulation of outcomes and costs. (B) Health states and Markov state transitions. Arrows indicate possible transitions between health states at each cycle, reflecting treatment remission, partial relapse or relapse for each intervention.

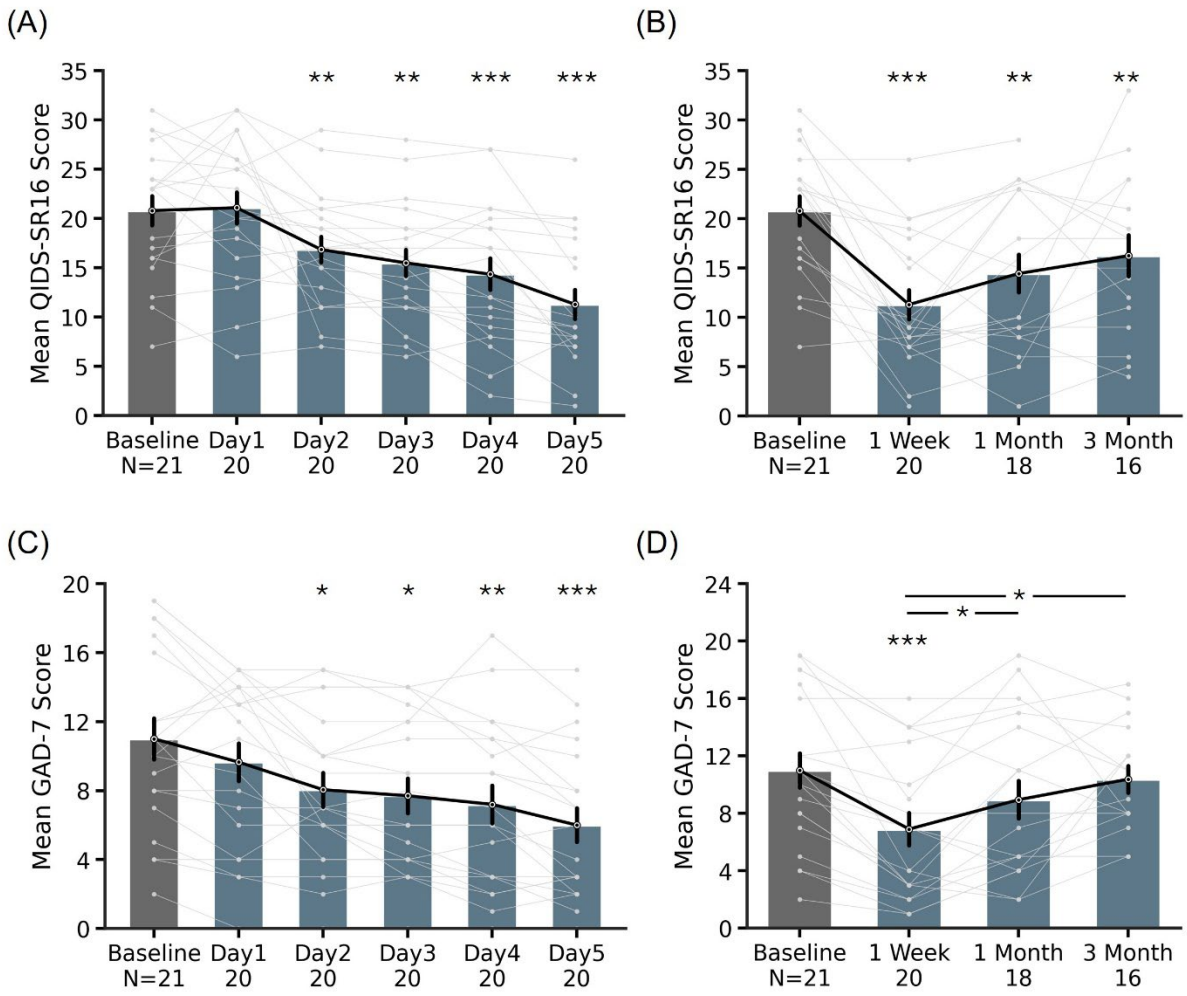

Figure S2. Longitudinal symptom trajectories during and after TAO-TMS treatment. (A) Mean QIDS-SR16 scores from baseline through each day of acute treatment (Day 1 to Day 5). (B) Mean QIDS-SR16 scores at baseline, post-acute treatment (1 week), 1-month, and 3-month follow-up. (C) Mean GAD-7 scores from baseline through each day of acute treatment (Day 1 to Day 5). (D) Mean GAD-7 scores at baseline, post-acute treatment (1 week), 1-month, and 3-month follow-up. Error bars represent standard error. * indicates statistical significance after multiple comparisons correction with FDR $q < 0.05$. *$p<0.05$. **<0.01. ***<0.001.

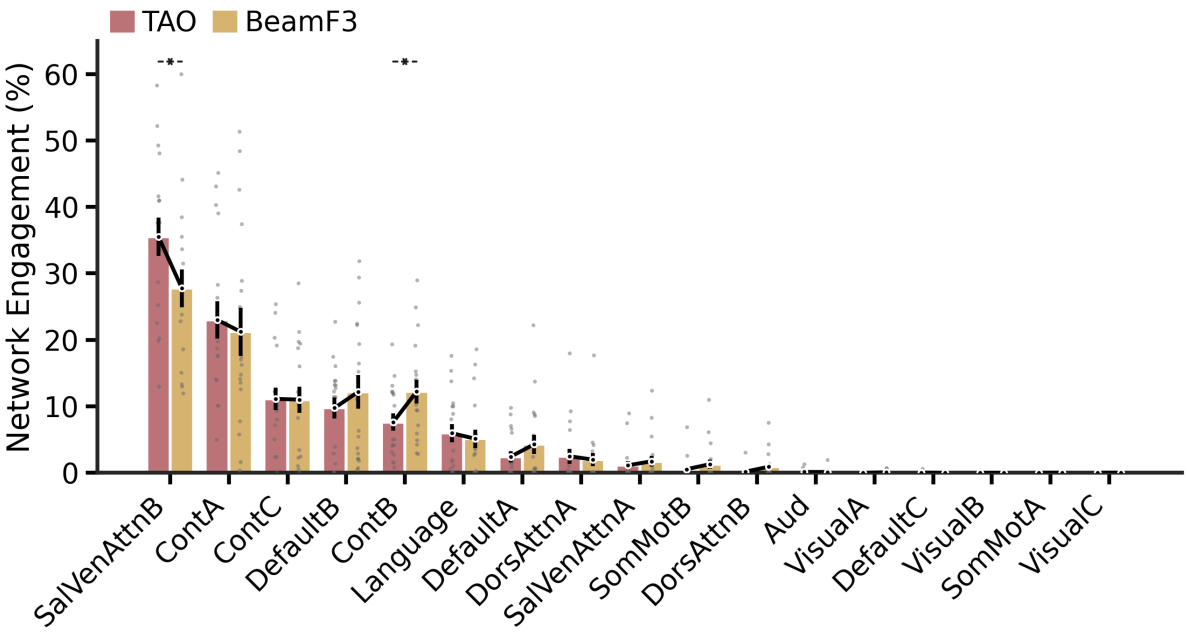

Figure S3. Network engagement of e-field hotspots for TAO-TMS and BeamF3 targets across large-scale cortical networks (Yeo et al., 2011; Kong et al., 2019).

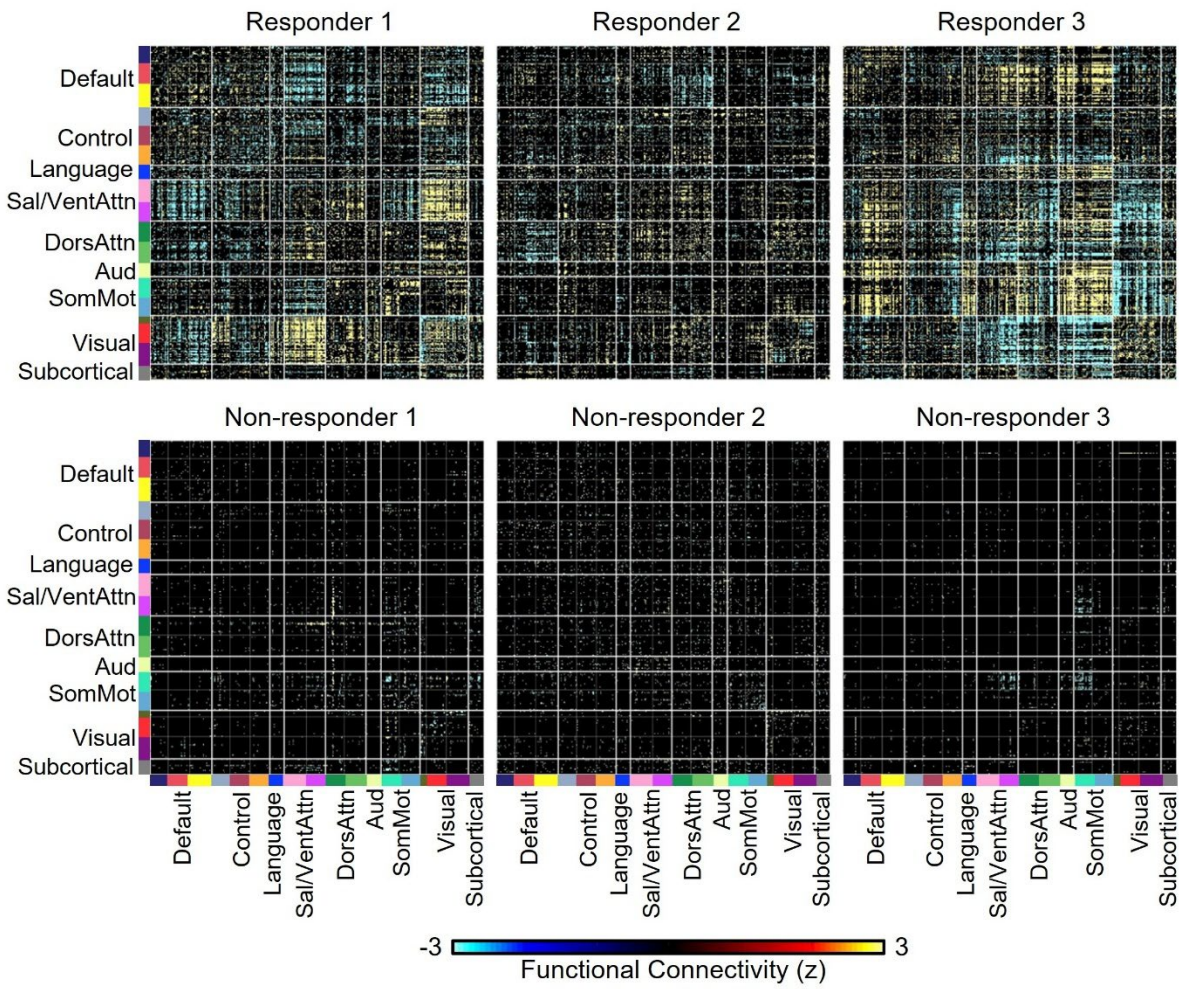

Figure S4. Thresholded functional connectivity (FC) change matrices for six participants. The 419 × 419 matrices show changes in FC from pre-treatment to post-treatment for three clinical responders and three non-responders, with edges surviving false discovery rate (FDR) correction at $p < 0.05$ highlighted.

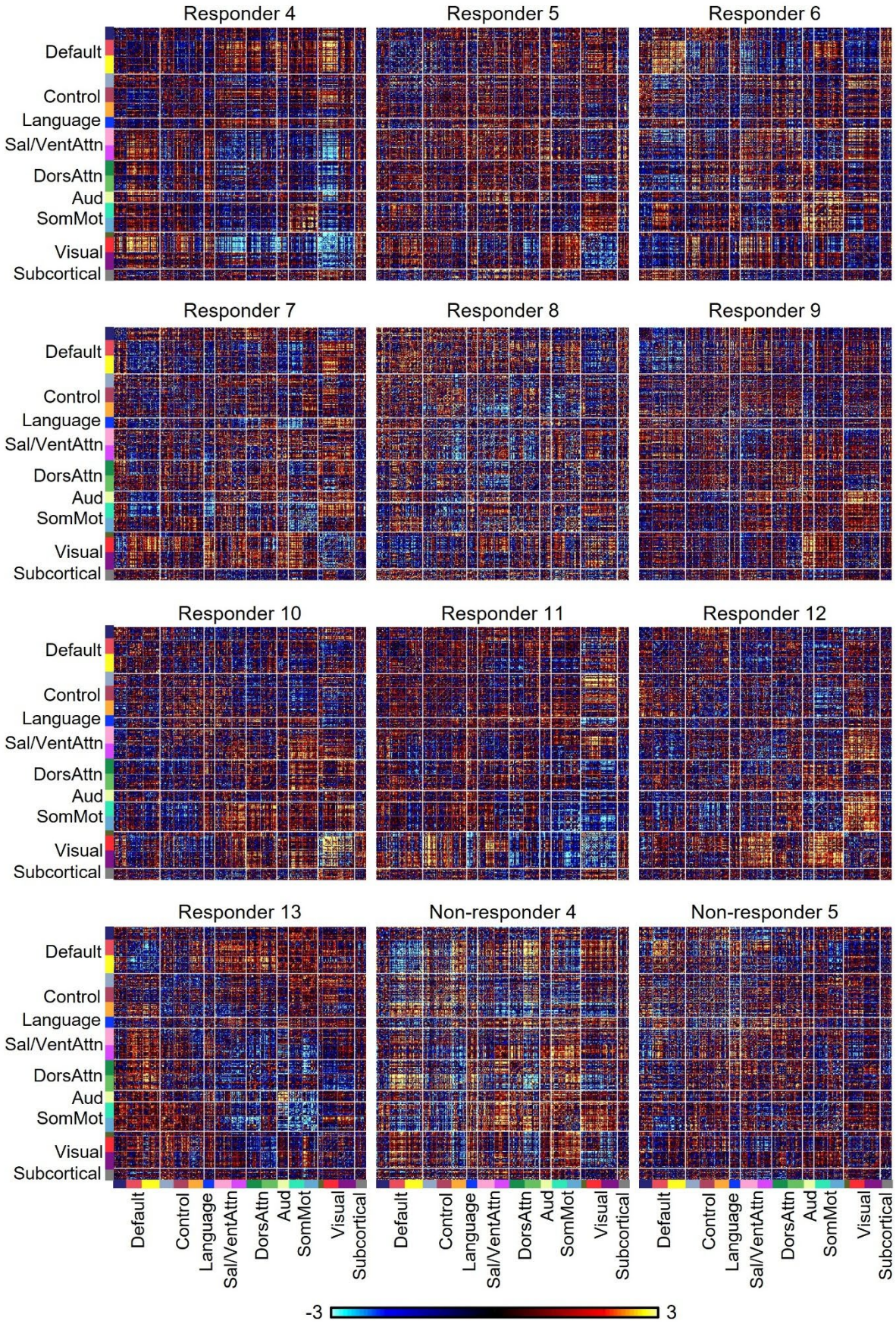

Figure S5. Functional connectivity (FC) change matrices of remaining participants.

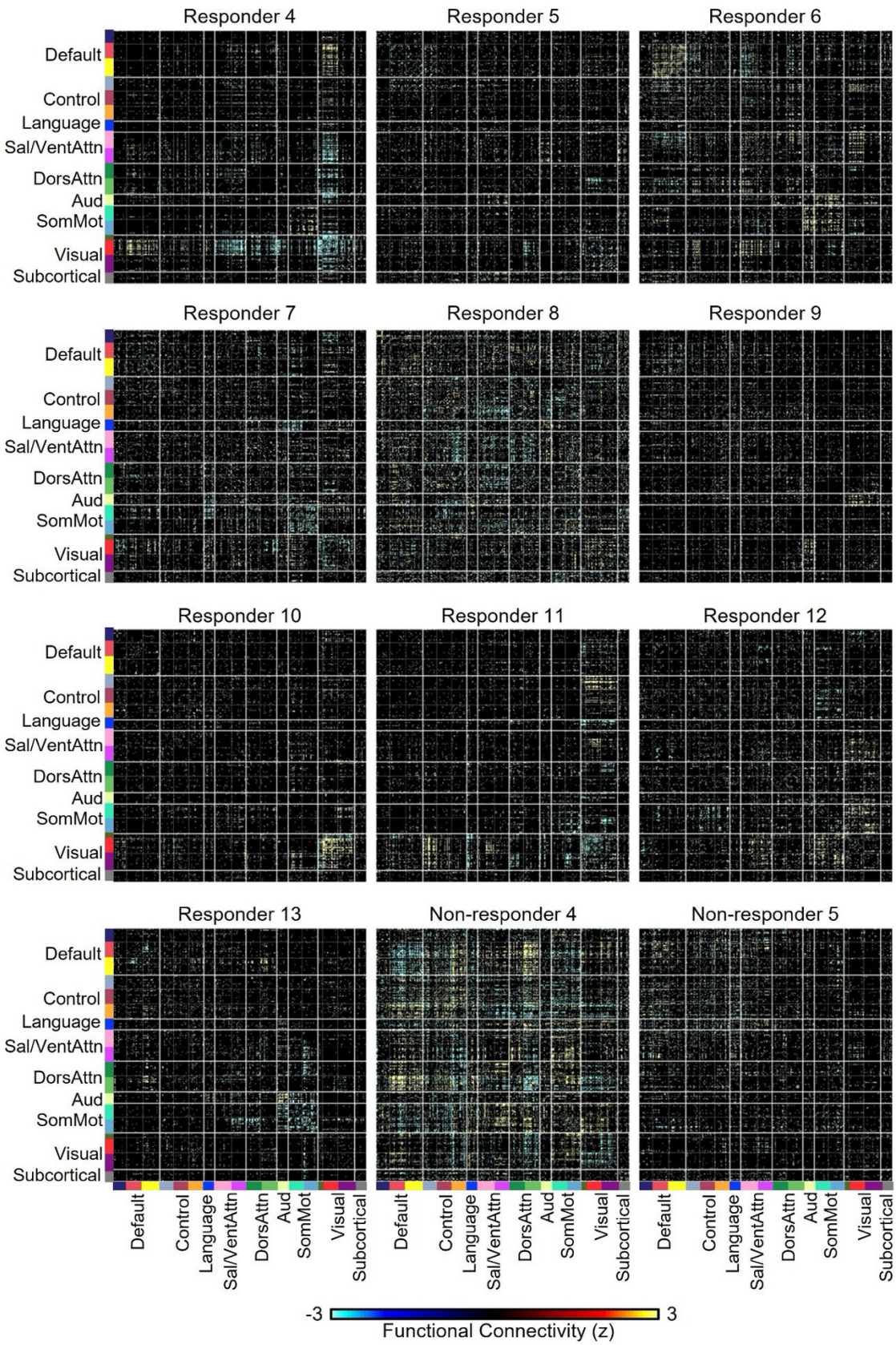

Figure S6. Thresholded functional connectivity (FC) change matrices of remaining participants, with edges surviving false discovery rate (FDR) correction at $p < 0.05$ highlighted.

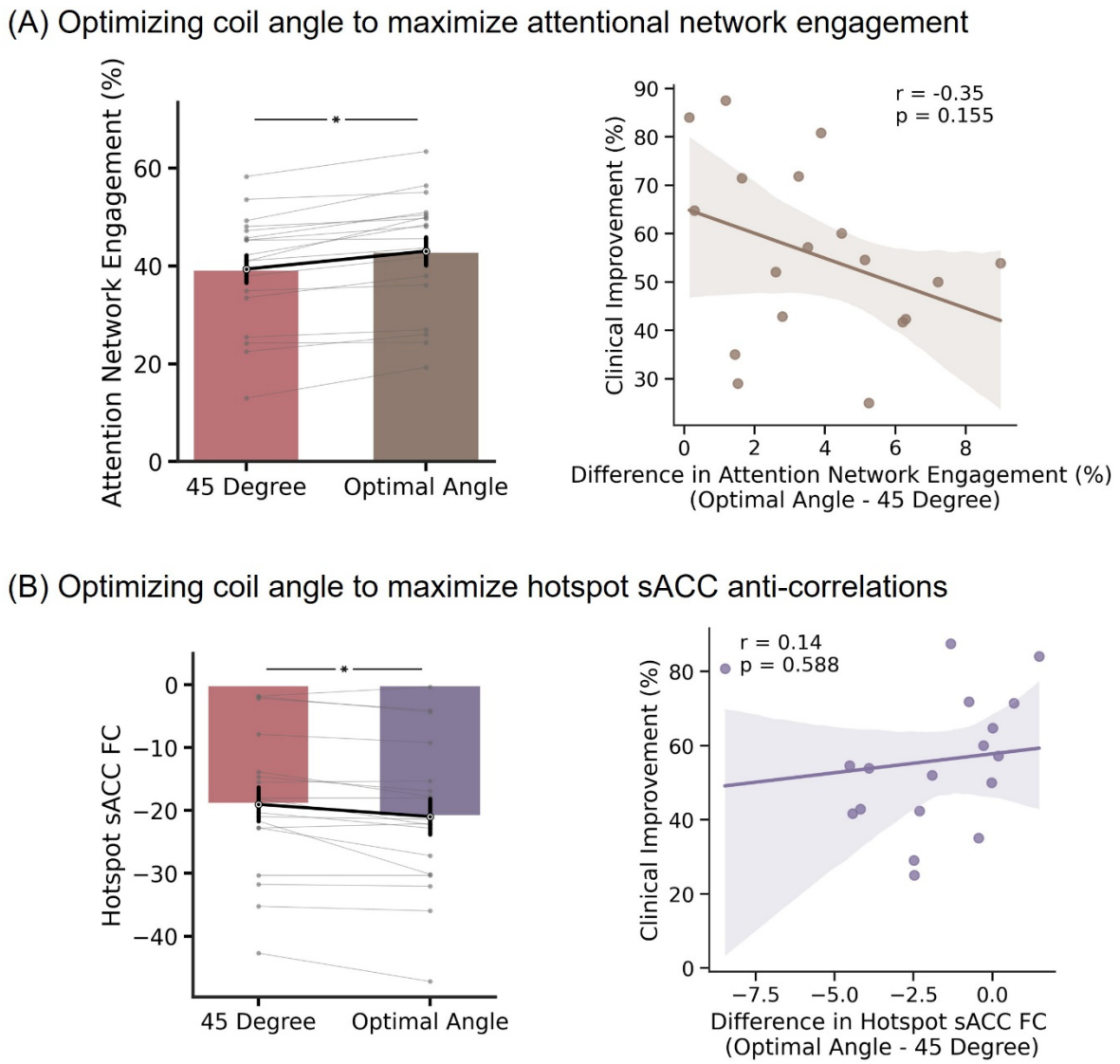

Figure S7. Post hoc exploratory analysis of the impact of coil orientation on clinical efficacy. (A) Optimizing coil angle to maximize attentional network engagement. The left panel shows the attention network engagement for the actual coil angle (45 degrees) and the optimal coil angle. The right panel shows the correlation of percentage MADRS reduction with the differences in on-target attentional network engagement between optimal and actual coil angles. A negative value would suggest that optimizing coil angle to maximize attentional network engagement might improve clinical efficacy. (B) Optimizing coil angle to maximize hotspot sACC anti-correlations. The left panel shows the hotspot sACC FC for the actual coil angle (45 degrees) and the optimal coil angle. The right panel shows the correlation of percentage MADRS reduction with the differences in hotspot sACC FC between optimal and actual coil angles. A negative value would suggest that optimizing coil angle to maximize hotspot sACC anti-correlations might improve clinical efficacy. Neither correlation reached statistical significance.

(A) Health system perspective

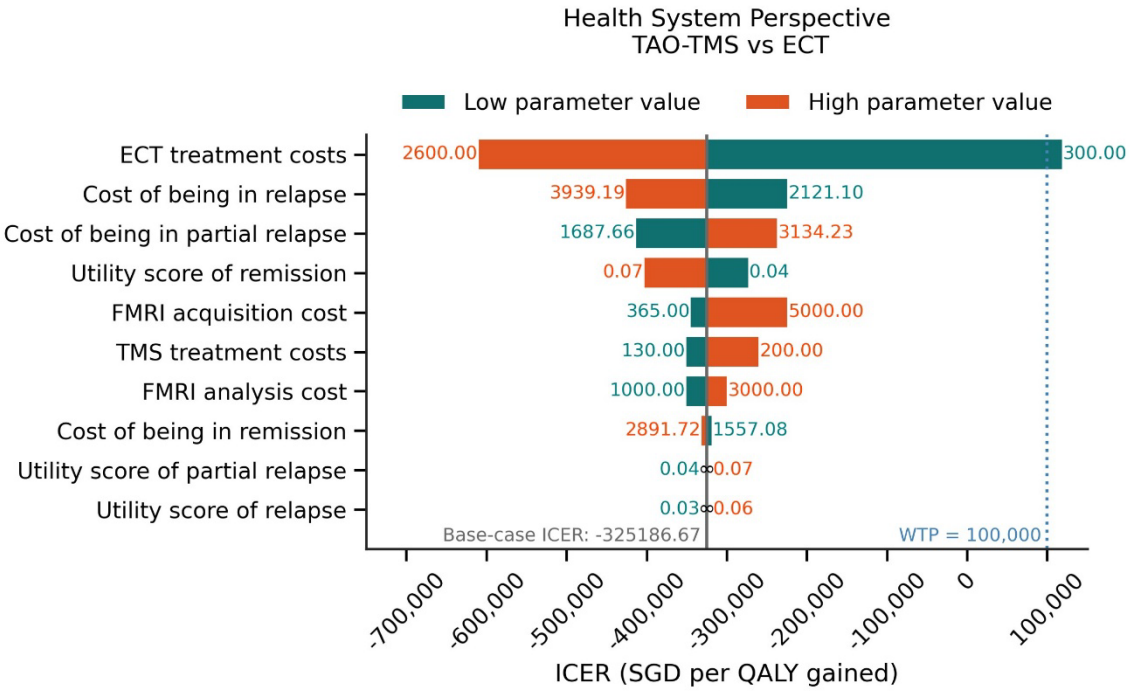

(B) Societal perspective

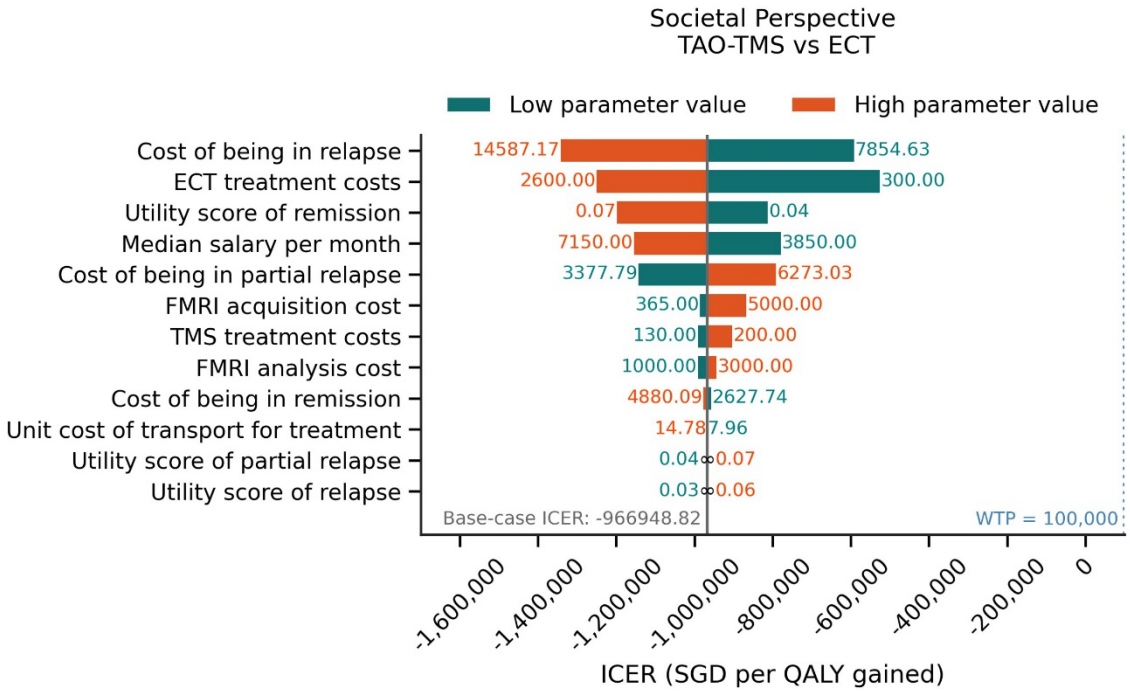

Figure S8. Tornado diagrams illustrating the results of one-way sensitivity analyses. The impact of individual input parameters on cost-effectiveness from (A) the health system perspective and (B) the societal perspective. Longer bars indicate greater influence of the parameter on the incremental cost-effectiveness ratio (ICER).

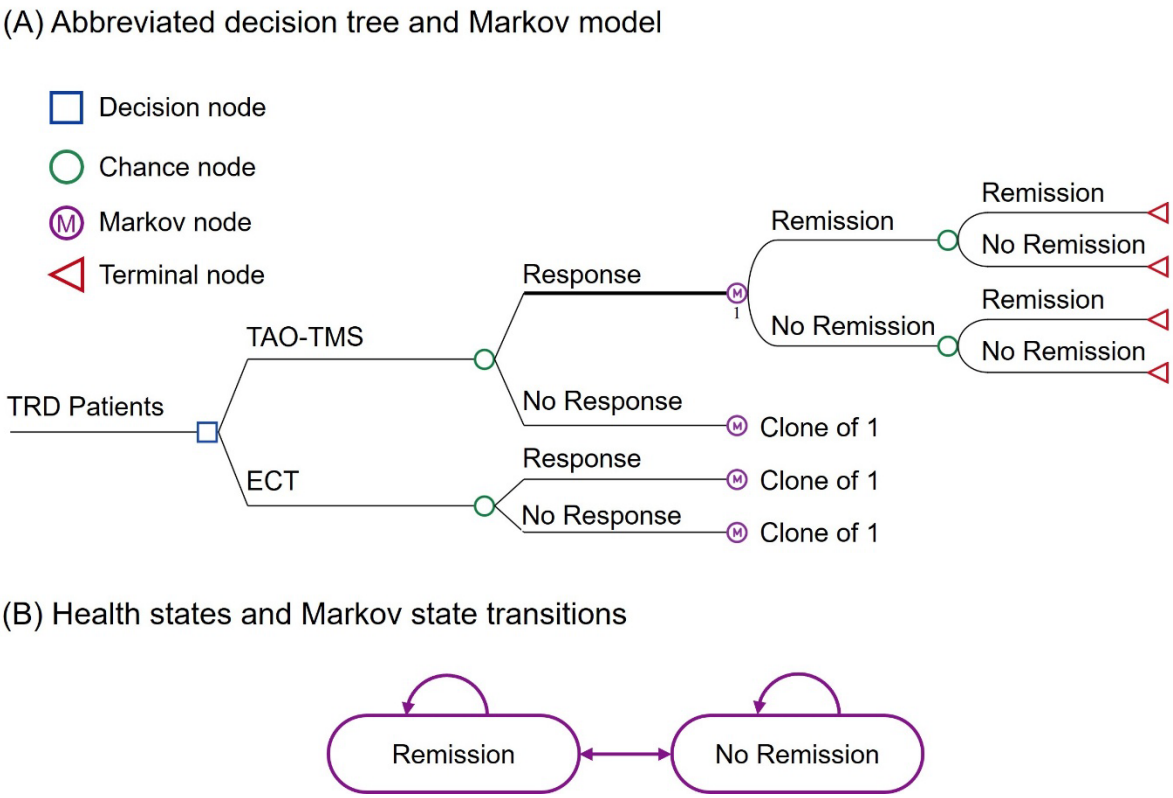

Figure S9. Decision analytical model comparing TAO-TMS and ECT for scenario analysis with two treatment responses and Markov health states. (A) Abbreviated decision tree and Markov model representing the clinical pathways for patients receiving TAO-TMS or ECT. Initial treatment decisions from the decision tree fed into the Markov model for long-term simulation of outcomes and costs. (B) Health states and Markov state transitions for two health states. Arrows indicate possible transitions between health states at each cycle, reflecting treatment remission or no remission for each intervention.

References

Avants, B.B., Tustison, N.J., Song, G., Cook, P.A., Klein, A., and Gee, J.C. (2011). A reproducible evaluation of ANTs similarity metric performance in brain image registration. NeuroImage *54*, 2033–2044.

Beam, W., Borckardt, J.J., Reeves, S.T., and George, M.S. (2009). An efficient and accurate new method for locating the F3 position for prefrontal TMS applications. Brain Stimul *2*, 50–54.

DuPre, E., Salo, T., Ahmed, Z., Bandettini, P.A., Bottenhorn, K.L., Caballero-Gaudes, C., Dowdle, L.T., Gonzalez-Castillo, J., Heunis, S., Kundu, P., et al. (2021). TE-dependent analysis of multi-echo fMRI with *tedana*. Journal of Open Source Software *6*, 3669.

Endicott, J., Nee, J., Harrison, W., and Blumenthal, R. (1993). Quality of Life Enjoyment and Satisfaction Questionnaire: a new measure. Psychopharmacology Bulletin *29*, 321–326.

Fischl, B. (2012). FreeSurfer. Neuroimage *62*, 774–781.

Fitzgibbon, K.P., Plett, D., Chan, B.C.F., Hancock-Howard, R., Coyte, P.C., and Blumberger, D.M. (2020). Cost-Utility Analysis of Electroconvulsive Therapy and Repetitive Transcranial Magnetic Stimulation for Treatment-Resistant Depression in Ontario. Can J Psychiatry *65*, 164–173.

Greve, D.N., and Fischl, B. (2009). Accurate and robust brain image alignment using boundary-based registration. Neuroimage *48*, 63–72.

Group, T.E. (1990). EuroQol-a new facility for the measurement of health-related quality of life. Health Policy *16*, 199–208.

Kong, R., Li, J., Orban, C., Sabuncu, M.R., Liu, H., Schaefer, A., Sun, N., Zuo, X.-N., Holmes, A.J., Eickhoff, S.B., et al. (2019). Spatial Topography of Individual-Specific Cortical Networks Predicts Human Cognition, Personality, and Emotion. Cereb. Cortex *29*, 2533–2551.

Li, J., Kong, R., Liégeois, R., Orban, C., Tan, Y., Sun, N., Holmes, A.J., Sabuncu, M.R., Ge, T., and Yeo, B.T.T. (2019). Global signal regression strengthens association between resting-state functional connectivity and behavior. NeuroImage *196*, 126–141.

Montgomery, S.A., and Åsberg, M. (1979). A new depression scale designed to be sensitive to change. The British Journal of Psychiatry *134*, 382–389.

Nasreddine, Z.S., Phillips, N.A., Bédirian, V., Charbonneau, S., Whitehead, V., Collin, I., Cummings, J.L., and Chertkow, H. (2005). The Montreal Cognitive Assessment, MoCA: a brief screening tool for mild cognitive impairment. Journal of the American Geriatrics Society *53*, 695–699.

Ooi, L.Q.R., Orban, C., Zhang, S., Nichols, T.E., Tan, T.W.K., Kong, R., Marek, S., Dosenbach, N.U.F., Laumann, T.O., Gordon, E.M., et al. (2025). Longer scans boost prediction and cut costs in brain-wide association studies. Nature *644*, 731–740.

Power, J.D., Mitra, A., Laumann, T.O., Snyder, A.Z., Schlaggar, B.L., and Petersen, S.E. (2014). Methods to detect, characterize, and remove motion artifact in resting state fMRI. Neuroimage *84*, 320–341.

Rush, A.J., Trivedi, M.H., Ibrahim, H.M., Carmody, T.J., Arnow, B., Klein, D.N., Markowitz, J.C., Ninan, P.T., Kornstein, S., and Manber, R. (2003). The 16-Item Quick Inventory of Depressive Symptomatology (QIDS), clinician rating (QIDS-C), and self-report (QIDS-SR): a psychometric evaluation in patients with chronic major depression. Biological Psychiatry *54*, 573–583.

Sheehan, D.V., Harnett-Sheehan, K., and Raj, B. (1996). The measurement of disability. International Clinical Psychopharmacology *11*, 89–95.

Spitzer, R.L., Kroenke, K., Williams, J.B., and Löwe, B. (2006). A brief measure for assessing generalized anxiety disorder: the GAD-7. Archives of Internal Medicine *166*, 1092–1097.

Yeo, B.T.T., Krienen, F.M., Sepulcre, J., Sabuncu, M.R., Lashkari, D., Hollinshead, M., Roffman, J.L., Smoller, J.W., Zöllei, L., Polimeni, J.R., et al. (2011). The organization of the human cerebral cortex estimated by intrinsic functional connectivity. Journal of Neurophysiology *106*, 1125–1165.

Zhao, Y.J., Tor, P.C., Khoo, A.L., Teng, M., Lim, B.P., and Mok, Y.M. (2018). Cost-Effectiveness Modeling of Repetitive Transcranial Magnetic Stimulation Compared to Electroconvulsive Therapy for Treatment-Resistant Depression in Singapore. Neuromodulation: Technology at the Neural Interface *21*, 376–382.